Next Generation Strategic Airlift Military Transport

AIAA Aircraft Design Competition

Paula Carsí de la Concepción

01/05/2015

Table of Contents

List of Figures

List of Tables

Notation

ABBREVIATIONS

AR:	Aspect ratio
c.g.:	Center of gravity
m.a.c:	Mean aerodynamic chord of the wing
MTOW:	Maximum take-off weight
RoC:	Rate of climb
TSFC:	Thrust specific fuel consumption

SYMBOLS

a:	Speed of sound
b:	Wing span
C:	Specific fuel consumption
e:	Efficiency factor
E:	Endurance
L/D:	Lift-to-drag ratio
M:	Mach number
q:	Dynamic pressure

R: Range
S: Wing reference area
T/W: Thrust-to-weight ratio
W/S: Wing loading ratio
V: Velocity

GREEK LETTERS
λ : Taper ratio
Λ: Sweep angle
ρ: Density
σ: Density ratio

SUBSCRIPTS
C_D: Drag coefficient
C_{D0}: Parasite drag coefficient
C_{Lmax}: Maximum coefficient of lift
C_{LTO}: Coefficient of lift at take-off
P_A: Power available
P_R: Power required
S: Wing area
S_a: Landing parameter
$S_{landing}$: Runway distance
T_R: Thrust required
T_{SL}: Thrust at sea level
W_0 : Take-off weight
W_1 : Weight at end of take-off segment
W_2 : Weight at end of climb segment
W_3 : Weight at end of cruise segment
W_4 : Weight at end of loiter segment
W_5 : Weight at end of land segment
W_e : Empty weight
W_f : Fuel weight

1. Introduction

The overall goal of this project is to design a next generation strategic airlift military transport for entry in 2030. The design must follow specific rules and specifications required by the AIAA Foundation Undergraduate Team Aircraft Design Competition.

1.1 Project Description

The final product of the project will be a proposal of no more than 100 double-spaced pages indicating all details and illustrations of the hypothetical aircraft. Requirements include, but are not limited to, minimizing fuel consumption for all missions, maximizing range for maximum payload, minimizing operating and fly away costs, and minimizing tie and ground track distance below

10,000 ft for optional tactical approach and landing. The aircraft is designed specifically towards fuel efficiency and cargo capacity/ease of loading and unloading. Next generation ideas for the years up until 2030 should also be considered.

The passage below consists of all the mission requirements. It was obtained from the AIAA competition design document.
'Mission Performance Requirements:

- 6,300 nm unrefueled range with a wartime planned load of 120,000 lb
- Maximum payload weight shall be no less than of 300,000 lb
- Cruise Mach number no less than 0.60
- Time to top of climb/climb to initial cruise altitude no more than 20 min with 205,000 lb
- Takeoff field length with maximum payload, and landing field length with maximum landing weight, no greater than 9,000 ft
- Takeoff, landing and climb requirements must be met at sea level in a ISA + 30 C day. Takeoff, and landing performance should also be shown at ISA + 10 C at 10,000' above MSL
- The aircraft shall be able to perform a takeoff, climb to pattern altitude, conduct pattern flight, and return to base with one or more engines out immediately after decision speed. Aircraft with an even number N of engines shall meet this requirement with any N/2 engine inoperative; if N is odd then assume N/2 + 1 engines inoperative. Indicate the maximum allowable increase in temperature and altitude over ISA sea level for which engine(s) out takeoff, as described here, can be met
- The aircraft shall be able to perform a tactical approach for arrivals to bases embedded in combat environments (see primary design objectives)
- Internal cargo volume, and corresponding cargo weight capacity, shall be no less than 44 463L master pallets, or one M104 Wolverine Heavy Assault Bridge

Other feature and considerations:

- The aircraft must be designed for minimal turn-around time, including: load and off load time, total cargo transfer time, servicing and refueling time
- Loading and unloading access must be demonstrated, with proper access doors, ramps, and clearances, for anticipated cargo units

Primary Design Objectives:

- Minimize fuel consumption for all missions
- Maximum range for maximum payload
- Minimize operating and fly away cost
- Minimize time and ground track distances below 10,000 ft for optional tactical approach and landing

Secondary Design Objective:

- Maximize cargo capacity in terms of number of units, without mixing, of the following (with consideration for weight and volume): M1A Abrams main battle tanks, M2/M3 Bradley Infantry Vehicles, Apache helicopters.

Notes and assumptions:

- Unless otherwise noted, assume standard atmosphere, and sea level for takeoff and landing
- Assume fuel reserves for a 200 nm radius (at optimal altitude for reserve cruise)

- No cruise altitude or Mach number is specified. Only level cruise segments may be considered, no cruise-climb is allowed. Cruise may be broken down to no more than 3 segments with altitude changes. Selection of all altitudes and timing of altitude changes within the cruise leg must be justified with proper analysis
- Climb speed shall not exceed 250 kts below 10,000 ft
- Assume production of 120 units
- Assume an EIS by 2030 for technology and concept assumptions'

1.2 Description of Team

OU Lead:
Dr. Alfred G. Striz, Professor
The University of Oklahoma
School of Aerospace and Mechanical Engineering
865 Asp Avenue, FH 206
Norman, Oklahoma, 73019-1052
Phone: 405-325-1730 Fax: 405-325-1088 striz@ou.edu

Chief Engineer:
Name: Paula Carsi de la Concepcion
Phone: (405) 778-5516
Email: cars3564@ou.edu
Area of Expertise: Controls

1.3 Team Time Schedule

The schedule (January to May, 2015) of the work is shown below with the left column displaying the first name and last name initials for each individual:

Week 2 – Week 5

Week 6 – Week 9

Week 10 –Week 13

Week 14 –Week 16

1.4 Summary of Effort to Date

01/19/2015 – 02/13/2015

- Configuration – blended wing body was selected to be the configuration of the aircraft
- Initial sketch – a sketch was draw for the initial design
- Initial weight estimation – the initial weight of the airplane was estimated using Raymer's method
- Airfoil selection & wing – airfoils were selected for the body and the wing
- T/W ratio and wing loading – thrust-to-weight ratio and wing loading were calculated
- Refined weight – the weight of the aircraft was calculated again using the more accurate method
- Cargo compartment – includes how to fit the cargo compartment in the body and dimensions of the cargo compartment
- Fuel system – locations and shapes of the fuel tanks
- Structures – structural consideration for the cargo compartment
- Engines – engine was selected for the aircraft based on mission requirements
- Special considerations: ramp and nose door and lift distribution

02/14/2015 – 03/13/2015

- New configuration – dimensions of the aircraft were changed
- Initial sketch, weight, and airfoil choice – new sketch was made for the aircraft, the weight was re-calculated and the airfoil was re-selected
- Calculated values for T/W ratio and wing loading – thrust-to weight ratio and wing loading were re-calculated
- Refined weight – refined weight was calculated using a more accurate method
- Cargo compartment and fuel system – more detailed considerations for the cargo compartment and fuel system
- Structures – more detailed structure consideration
- Engines – a new engine was selected because the changed design of the aircraft
- Special considerations

03/14/2015 – 4/10/2015

- CAD model – a CAD model was created using SolidWorks
- Cost analysis – calculations of the costs for this project
- Special aerodynamic considerations – considerations for unexpected separation of the flow and unwanted vortex
- Stability calculations – calculations regarding flight controls
- Flight mechanics calculations – calculations of lift, drag and performance of the aircraft
- Wing loading re-calculation

04/10/2015 – 05/04/2015

- Flight mechanics calculations continued

- Landing gear – the locations of front and rear landing gears, the number of landing gears, and the way to store these landing gears
- Solidification of engine – finalizing the engine selection and thrust calculations if necessary
- Fuselage structural analysis – continued structural analysis
- Doors and cockpit analysis – detailed design of the doors, ramps, and the cockpit

1.5 Work Left To Be Done (Action List)

- Preliminary design – more refined and detailed design after the basic design
- Prototypes manufacturing – prototypes will be built for testing
- Flight test – develops and gathers data during flight of prototypes in order to validate the design
- Design modifications – modifications will be made based on analysis of the data obtained during flight test

2. Project Activities

2.1 Literary Search

See the reference section at the end of the report. The majority of the literary sources used was for determining specific methods of calculating values necessary for the aircraft. Integration of different methods with the specific shape and structure of the design elaborated on below was obtained from the references. The references included but was not limited to various internet sources, textbooks and online/offline journal articles.

Specifically, the journal article by Mukhopadhyav over the triple bubble design for the structure of the aircraft, the texts books by Raymer and Nikolai for calculations of simple designs, and the case study of the C-5 from AIAA were the most integral parts of the literary information necessary to complete the project. The triple bubble design is what allows the BWB to be structurally sound. Raymer and Nikolai act as the guidelines for calculations including initial weight, sizing of the wing, and R&D costs. And finally the case study was used as a historical reference.

2.2 Notes on Brainstorming Sessions, Internal and External Communications

First, several meetings were reserved for brainstorming/Figures of Merit discussion. No ideas were turned away, and discussions were held regarding the feasibility of any and all ideas. In the next several meetings, discussions of the ideas went into detail to determine a configuration. Configurations considered ranged from a conventional H-tail aircraft to a flying wing.

Then, some meetings were dedicated to determining the distribution of work. The last few meetings consisted of putting together the work done so far, checking for coherence of data and missing information. A final meeting was needed to finish formatting the report.

3. Disciplinary Investigations

3.1 Configuration of Overall Design

The configuration of this next generation strategic airlift military transport will be a blended wing body. Although the conventional configuration is more convenient to load and unload, a blended wing body was chosen because for the following reasons. The blended wing body transport has an airfoil shaped body and its wings are smoothly blended into the body. Compared to the conventional configuration, the blended wing body has a smaller surface area, thus, it has lower drag. Both the body and the wings provide lift during flight. With a high lift-to-drag ratio, it has high fuel efficiency as well as long range.

A simple figure of merit, as shown in Table 1, which was based on various factors from aesthetics to uniqueness was used to determine the pathway for aircraft configurations to pursue.

Table 1: Figure of Merit for Configuration Choice

Designs (1-5)	Conv. Aircraft (H-Tail)	Weighted Score	Blended Wing Body	Weighted Score	Flying Wing	Weighted Score
Uniqueness (3)	2	6	4	12	5	15
Aerodynamic Efficiency (3)	2	6	4	12	5	15
Structural Soundness (3)	4	12	3	9	1	3
Aesthetic Appeal (1)	2	2	5	5	2	2
Historical Data (2)	4	8	1	2	2	4
Loading/Unloading (1)	4	4	3	3	2	2
Cargo Compartment (3)	3	9	4	12	1	3
Sum		47		55		44

Size Determination:

At the beginning of the designing process it is important to have historical data from similar aircraft as a basis. These data may also help in identifying how values change depending on the design. Research about current military cargo aircraft shows that all of them have similar configurations: long and strong fuselage, enormous wings and a large T-tail or H-tail. However, finding data about BWB aircraft for military cargo applications is near impossible due to the lack of such aircrafts. Essentially, they are a new concept in this field. The current military cargo aircraft that are close to the present design requirements have been summarized in Table 4, including weight, payload, range, and sizing data.

Table 2: Sizing Research

	C-5 GALAXY	C-17	AN-225	AN-224
Tail	T-Tail	T-Tail	Twin Tail, Large H Stabilizer	Cross Tail
Wing Sweep	25 deg			
Cargo Compartment	121l x 13.5h x 19w	88l x 12.4in h x 18w	142.2l x 14h x 21w	118l x 14h x 21w
Cargo Volume	31000 ft^3		46000 ft^3	
Pallets	36	18		
Payload	270000 lb	170000 lb	560000 lb	330000 lb
Length	247 ft 1 in	174	275 ft 7 in	226ft 3in
Wingspan	222 ft 9in	170	290 ft	240ft 5 in
Height	65 ft 1 in	55.1 ft	59 ft 5 in	68ft 2 in
Wing Area	6200 ft^2	3800 ft^2	9740 ft^2	6760 ft^2
MTOW	840000 lb	585000 lb	1410000 lb	893000 lb
Max Speed	0.79		459 kn 0.8	467 kn
Cruise Speed	0.77	0.74	432 kn 0.753	430 kn 0.75
Range	2400 nm w/ 263200lb	2800 nm w/ 160000lb	8315	6000 nm
Fuel Capacity	51150 us gal	35546 us gal	300000 kg	
T/W	0.22	0.277	0.234	0.23
W/S	120 lb/ft^2	150 lb/ft^2	135.8 lb/ft^2	74.7 lb/ft^2

From Table 2, it is easy to see that only the AN-225 can carry a heavier payload than the requirements for the new military aircraft, but the range is shorter in comparison. That means that the new design has to be bigger than most current military cargo aircraft, with large payload and increased range. Thus, the configuration that makes the most sense seems to be a blended wing body aircraft.

3.2 Sketch of Design

The transport aircraft was modeled using CAD software. The aircraft is a blended wing body configuration. The driver for the size of the aircraft is the cargo volume necessary to perform all mission requirements.

Figure 1: Isometric View of the Conceptual Design of the Aircraft

The dimensions of the aircraft are discussed in the sections to come in addition to a three view model. All relevant dimensions are displayed in feet.

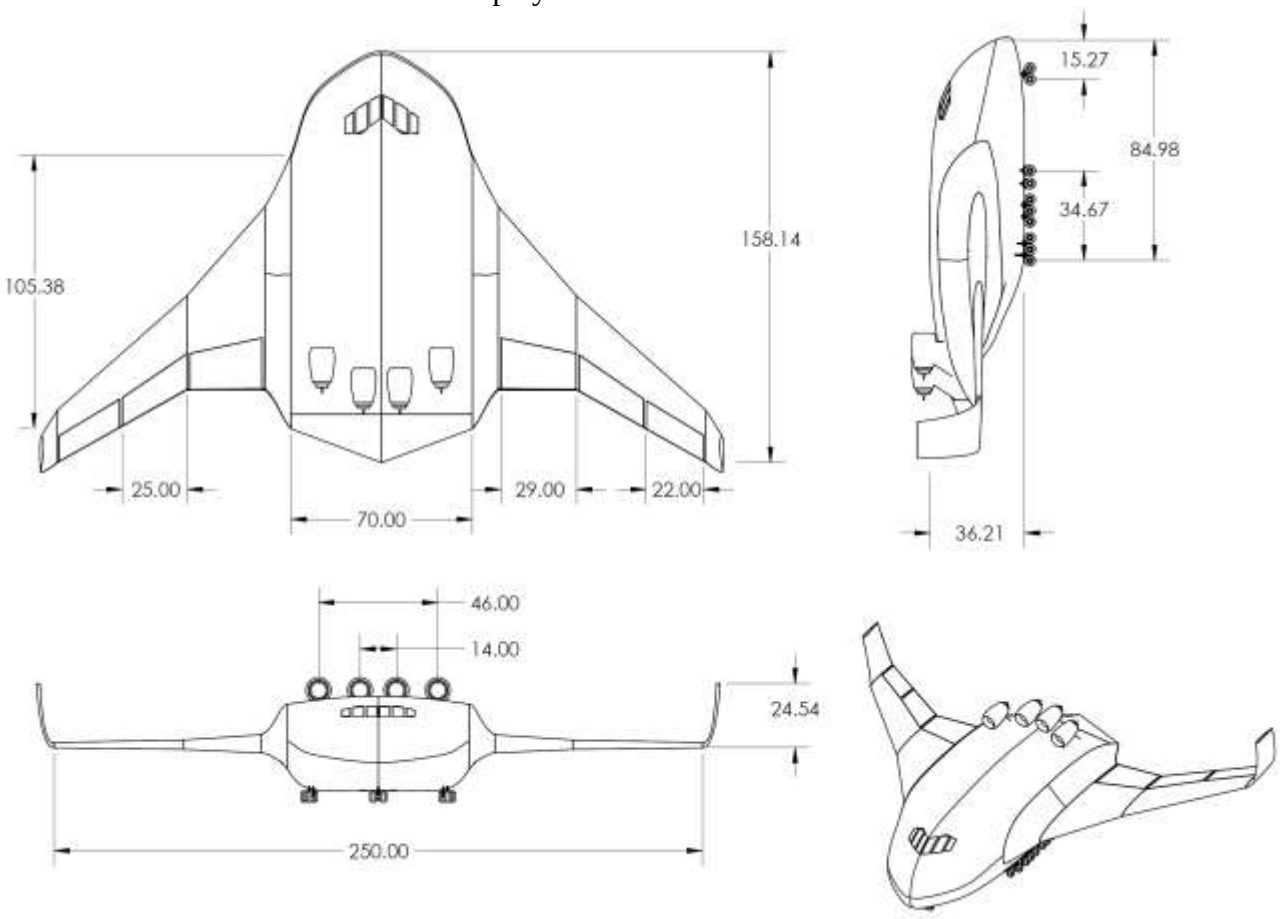

Figure 2: Three View Drawing of Aircraft Design

3.3 Initial Weight Estimation of Design

Starting with an estimated aspect ratio of 4 determined from initial sketches and a S_{wet}/S_{ref} ratio of 2.2 determined from historical trends, the resulting wetted aspect ratio came out to be 1.82. Using this wetted aspect ratio, the L/D_{max} was determined from a plot of various BWB L/D values versus MTOW. The value attained was 22 for loiter and 19.052 for cruise. The specific fuel consumption values for the cruise and loiter mission segments of the aircraft were chosen for a high bypass turbofan engine, thus setting the values at 0.5 and 0.4 respectively. Knowing the unrefueled range as 6,300 nm at a wartime planned load of 120,000 lb, the cruise fuel weight fraction may be calculated using Eq. 1. Similarly, assuming the endurance is 1800 s^{-1}, the loiter fuel weight fraction may be calculated using Eq. 2.

$$\frac{W_x}{W_{x-1}}(cruise) = e^{-\frac{RC}{V(\frac{L}{D})}} \quad (1)$$

$$\frac{W_x}{W_{x-1}}(loiter) = e^{\frac{EC}{\frac{L}{D}}} \quad (2)$$

Assuming a standard cargo mission of warmup/take-off followed by climb, cruise, loiter, and land, the mission segment weight fractions may be summed up in Table 3:

Table 3: Collection of Mission Fuel Fractions

Mission Number	Mission Name	W_x/W_0
1	Warmup/Take-off	0.970
2	Climb	0.985
3	Cruise	0.728
4	Loiter	0.988
5	Land	0.995

Factoring in fuel reserves, the fuel weight fraction is calculated using Eq. 3 to be 0.335.

$$\frac{W_f}{W_0} = 1.06\left(1 - \frac{W_5}{W_0}\right) \quad (3)$$

Then for the empty weight fraction, Eq. 4 was used considering the aircraft is a military cargo/bomber.

$$\frac{W_e}{W_0} = 0.93W_0^{-0.07} \quad (4)$$

Eq. 5 was iterated until the final weight of 1,050,000 lb was obtained.

$$W_0 = \frac{120{,}000}{1-\frac{W_f}{W_0}-\frac{W_e}{W_0}} \quad (5)$$

3.4 Airfoil Selection

For the wings, the NACA 1410 airfoil was selected, and is shown in the figure below. It has the ability to provide enough lift to the aircraft and it gives reasonable drag at the same time. The NACA SC(2)-0714 supercritical airfoil was also considered; however, its lift coefficient is too high compared to normal airfoils, which caused problems with the sizing of the wings along with various other calculations.

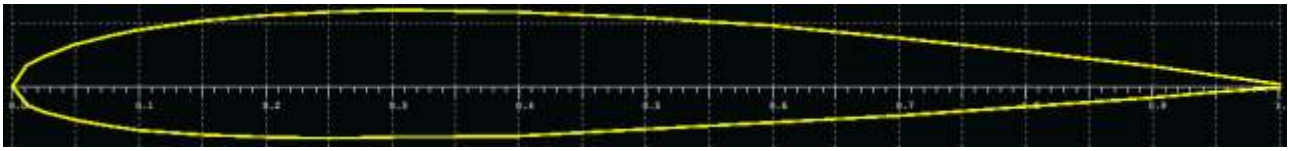

Figure 3: NACA 1410

For the NACA 1410 airfoil:

- Max thickness: 10% at 29.9% chord
- Max camber: 1% at 50% chord
- Max lift coefficient: 2.1

The lift coefficient vs. angle of attack and the drag coefficient vs. angle of attack of the airfoil are shown in Figure 1. The lift-to-drag ratio vs. angle of attack is shown in Figure 2.

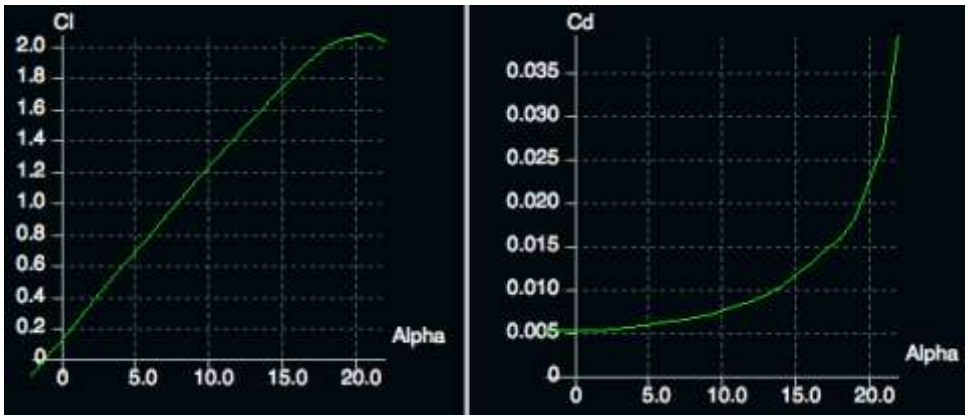

Figure 4: Lift Coefficient and Drag Coefficient vs. Angle of Attack of the Airfoil

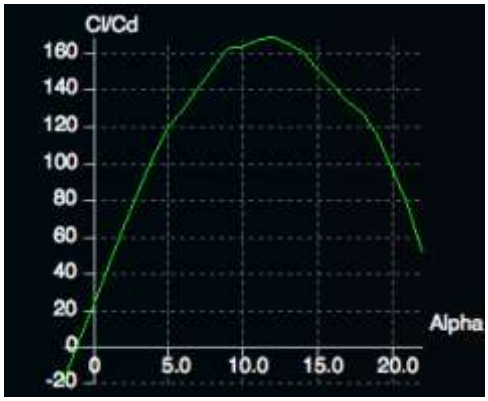

Figure 5: Lift-to-Drag Ratio vs. Angle of Attack of the Airfoil

3.5 Thrust-to-Weight Ratio Calculations

Thrust-to-weight ratio (T/W) is a key factor in the performance of any aircraft. Thrust-to-weight ratio drives how an airplane will behave when accelerating, climbing, reaching maximum speed, and turning. For conceptual design, thrust-to-weight ratio is referred as the ratio given for static, sea-level thrust.

Table 5.1 presented in 'Aircraft Design: A Conceptual Approach' by Daniel Raymer offers a list of typical values of ratios for different types of aircraft.[15] For this transport aircraft, a desired and acceptable ratio will lie between 0.2 and 0.27.
Thrust-to-weight ratio has been analyzed statistically over many years of aerospace engineering design, resulting in a model based on the desired cruise Mach number, which is given in Eq. 6.

$$\frac{T}{W_o} = aM_{\mathrm{m}}^{c} \tag{6}$$

where M_m is the maximum Mach number and a and c are statistical model constants provided by Raymer in Table 5.3. Given an expected Mach number of 0.8, the statistical thrust-to-weight ratio corresponding to this speed is 0.23.

Comparison Analysis:
Taking into consideration the thrust-to-weight ratio yielded by this statistical analysis, the configuration of the aircraft was compared directly with several airplanes with either similar configuration, or similar mission specifications.

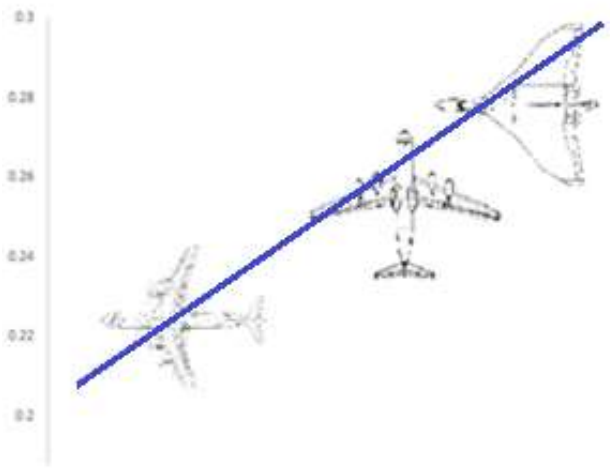

Figure 6: Thrust-to-Weight Ratio of Different Aircrafts

It was decided that the most important factor of the configuration of the aircraft was its transport capability, thus, making that the most influential category when choosing a thrust-to-weight ratio by comparison. Ultimately, it is for that reason that the present thrust-to-weight ratio lies closer to that of the transport aircraft instead of the values given for aircraft of similar configurations, such as the Avro Vulcan.

Thrust-to-Weight Selection:
The thrust-to-weight ratio for the transport aircraft was set to be 0.23 in order to allow the desired performance at cruise altitude. It is justifiably an acceptable value since both statistical analysis and comparison analysis yielded similar results.

Thrust-to-Weight Ratio for Different Flight Conditions:
Based on the value chosen for the static sea level thrust-to-weight ratio, the thrust-to-weight ratios for different flight configurations can be found. Thrust-to-weight ratio can be calculated as given in equation 5.2 from Raymer's 'Aircraft Design'.

$$\left(\frac{T}{W}\right)_i = \frac{1}{\left(\frac{L}{D}\right)_i} \tag{7}$$

Where (T/W) is the thrust-to-weight ratio for an i condition, and (L/D) is the lift-to-drag for the same i condition. Such equation yields results that can be used to estimate the thrust-to-weight ratio for cruise conditions, loiter conditions, and take of conditions. In the case of climb the equation gets modified as follows,

$$\left(\frac{T}{W}\right)_{climb} = \frac{1}{\left(\frac{L}{D}\right)_{climb}} + \frac{V_{vertical}}{V} \tag{8}$$

In the case of the transport aircraft, some thrust-to-weight ratios are given in the Table 4.

Table 4: Thrust-to-Weight Ratios for Different Altitudes

Description	T/W
Cruise (36,000 ft)	0.07
Loiter	0.05
Climb	0.11
Take-off	0.08
SLUF 10,000 ft	0.07
SLUF 20,000 ft	0.07
SLUF 30,000 ft	0.06
SLUF 40,000 ft	0.04

3.6 Wing Loading Calculations

The lowest wing loading (W/S) was selected after calculating multiple different wing loadings for several different flight conditions. The flight conditions included in the initial wing loading estimate are stall, take-off, landing, cruise, endurance, instantaneous turn, sustained turn, and max ceiling. All of the preliminary calculations were found using equations from Raymer.[15] The stall W/S equation is as follows:

$$\frac{W}{S} = \frac{1}{2}\rho_{cruise} V_{stall}^2 C_{Lmax} \tag{9}$$

The take-off W/S equation is as follows, with TOP as Take-off parameter, sigma as the density ratio, a T/W ratio found using an initial guess, and the lift coefficient at take-off:

$$\frac{W}{S} = (TOP)\sigma C_{LTO}\frac{T}{W} \tag{10}$$

The landing distance W/S equation is as follows, with $S_{landing}$ as the runway distance, and S_a as a landing parameter:

$$\frac{W}{S} = \frac{(S_{landing} - S_a)\sigma C_{Lmax}}{80} \tag{11}$$

The cruise W/S equation is as follows with q as dynamic pressure, A as aspect ratio, e as the efficiency factor, and C_{Do} as the parasite drag coefficient:

$$\frac{W}{S} = q\sqrt{\pi Ae C_{Do}/3} \tag{12}$$

The endurance W/S equation is as follows:

$$\frac{W}{S} = q\sqrt{\pi Ae C_{Do}} \tag{13}$$

The instantaneous turn W/S equation is as follows with n as the load factor:

$$\frac{W}{S} = \frac{qC_{Lmax}}{n} \tag{14}$$

The sustained turn W/S equation is as follows:

$$\frac{W}{S} = \frac{q}{n}\sqrt{\pi Ae\ C_{Do}} \tag{15}$$

The maximum ceiling W/S equation is the same as the endurance equation. The wing loading for the blended wing body was lowest for the landing distance calculation. A wing loading of 68.03 lb/ft^2 was calculated as the lowest wing loading. This wing loading value was set in a ratio with the gross take-off weight to obtain an estimated wing area. Table 5 exhibits all the values for the different wing loadings at different flight conditions.

Table 5: Wing Loading Values at Specific Flight Conditions

Wing Loading	
Stall:	92.30
Takeoff:	68.03
Landing Dist.:	117.60
Cruise:	94.93
Endurance:	164.43
Inst. Turn:	838.40
Sustained Turn:	164.43
Max Ceiling:	164.43

3.7 Refined Weight Estimation of Aircraft

Knowing the T/W ratio and W/S ratio, a new resized weight may be calculated. Considering the aircraft as a military cargo/bomber, the new empty weight fraction may be determined using the equation in Table 6 from Raymer:

Table 6: Resized Weight Calculation Constants

$$W_e/W_0 = (a + bW_0^{C1}A^{C2}(T/W_0)^{C3}(W_0/S)^{C4}M_{max}^{C5})K_{us}$$

	a	b	$C1$	$C2$	$C3$	$C4$	$C5$
Jet trainer	0	4.28	−0.10	0.10	0.20	−0.24	0.11
Jet fighter	−0.02	2.16	−0.10	0.20	0.04	−0.10	0.08
Military cargo/bomber	0.07	1.71	−0.10	0.10	0.06	−0.10	0.05
Jet transport	0.32	0.66	−0.13	0.30	0.06	−0.05	0.05

K_{VS} = variable sweep constant = 1.04 if variable sweep
= 1.00 if fixed sweep

Iterating the above formula yielded a new resized maximum take-off weight of 950,000 lb. This was done using the assumption that the crew would consist of five people each with an average of 250 lb together with their luggage and a thrust to weight ratio of 0.23.

3.8 Cargo Compartment

Cargo Required:
One of the most important aspects of the design is to make sure that the cargo requirements are met. Thus, it is important to know all the dimensions of all the different cargo that must be carried in the aircraft. These dimensions are pertinent to the maximum width, length and height of the cargo bay in the aircraft.

1. Wolverine Bridge – Armored military engineering vehicle created to allow ground military units to traverse normally non-traversable terrain i.e. ditches, broken bridges, etc.

Table 7: Wolverine Bridge Dimensions

Dimensions	Quantity	Units
Length	44	ft
Width	13	ft
Height	13	ft
Weight	153,883	lb

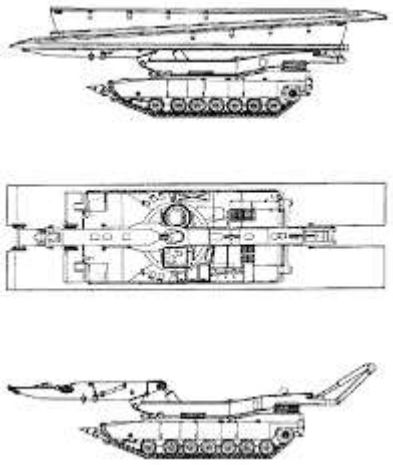

Figure 7: Wolverine Bridge Illustration

2. Apache Helicopter – Four-blade, twin-engine attack helicopter with a tandem cockpit for a two-man crew.

Table 8: Apache Helicopter Dimensions

Dimensions	Quantity	Units
Length	49	ft
Width	17	ft
Height	12.9	ft
Weight	11,390	lb

Figure 8: Apache Helicopter Illustration

3. Chinook Helicopter – Twin-engine tandem rotor heavy-lift helicopter. Used for troop movement, artillery placement and battlefield resupply.

Table 9: Chinook Dimensions

Dimensions	Quantity	Units
Length	58	ft
Width	13	ft
Height	18	ft
Weight	23,400	lb

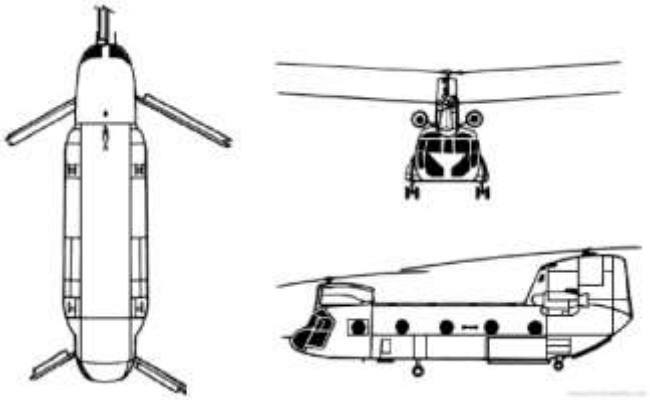

Figure 9: Chinook Helicopter Illustration

4. 44 463L Master Pallets – Standardized pallets used for transporting military air cargo. Designed to be loaded and offloaded on military/other cargo aircrafts.

Table 10: 463L Master Pallet Dimensions

Dimensions	Quantity	Units
Length	9	ft
Width	7.33	ft
Height	0.33	ft
Weight	290	lb

Figure 10: Master Pallets Illustration

5. M1A2 Abrams Tank – An American main battle tank that is heavily armed and armored. It is one of the heaviest tanks in service.

Table 11: M1A1 Abrams Tank Dimensions

Dimensions	Quantity	Units
Length	32	ft
Width	12	ft
Height	8	ft
Weight	136,000	lb

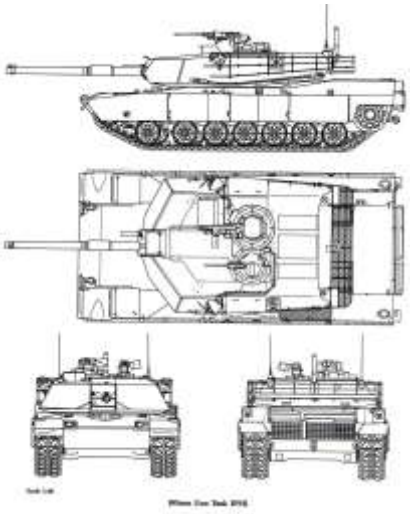

Figure 11: M1A1 Abrams Tank Illustration

Cargo Compartment:
Taking into account that the new generation cargo aircraft has to increase the cargo capacity from the current ones, and considering the maximum dimensions of the required cargo objects, the cargo compartment can be designed.

The cargo compartment will be able to contain:

- 3 Apache Helicopters
- 2 Apache Helicopters and 1 Chinook Helicopter
- 2 Abram Tanks
- 44 436L Master Pallets
- 2 Wolverine Bridges

The blended wing body configuration can have a large amount of cargo space as the cargo compartment fills the large center wing body section wings. Also, due to the shape of the blended wing body, the cargo compartment is not restricted to a cylindrical shape.

Table 12: Cargo Compartment Dimensions

Dimensions	Quantity	Units
Length	69.2	ft
Width	60.0	ft
Height	21.1	ft

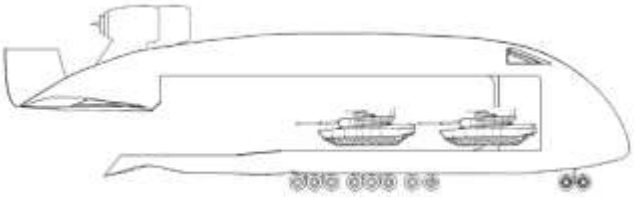

Figure 12: Side View of Abram Tanks

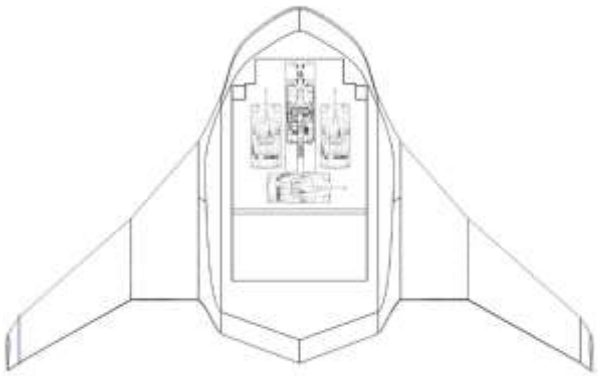

Figure 13: Top View of Abram Tanks

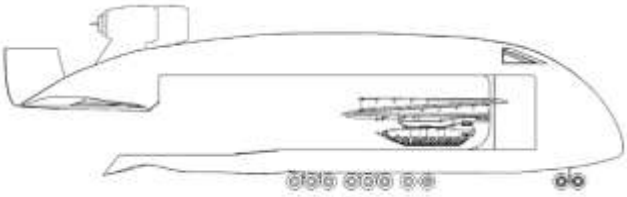

Figure 14: Side View of Wolverine Bridge

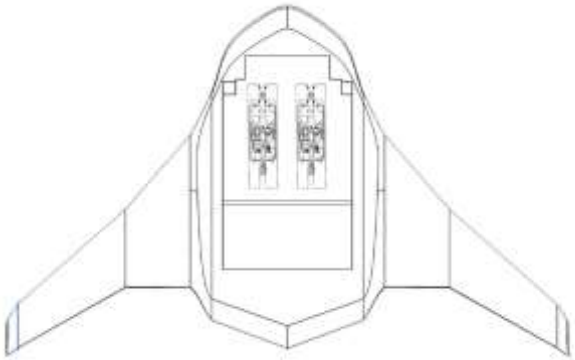

Figure 15: Top View of Wolverine Bridge

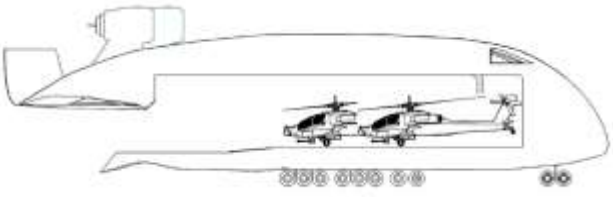

Figure 16: Side View of Apache Helicopter

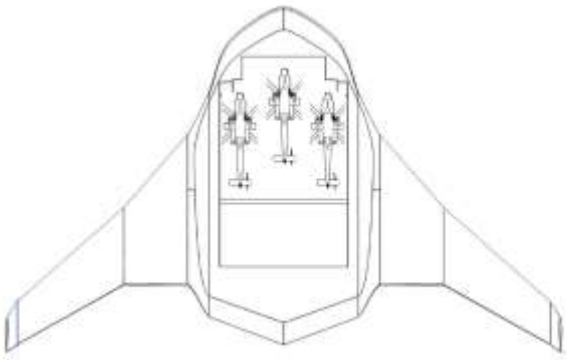

Figure 17: Top View of Apache Helicopter

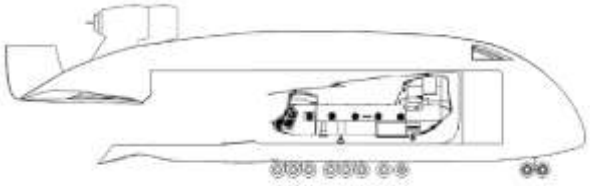

Figure 18: Side View of Chinook Helicopter

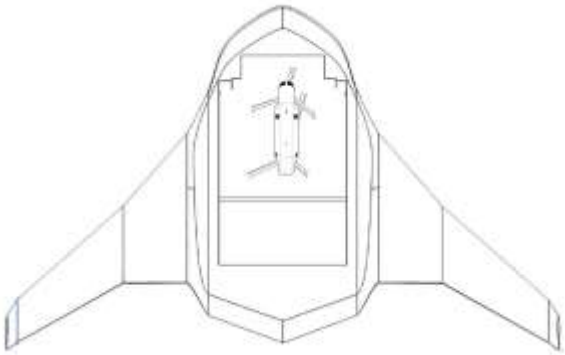

Figure 19: Top View of Chinook Helicopter

3.9 Main Body Design

The shape of the body of this next generation strategic airlift military transport is shown in Figure 13. The rear part of this shape is inspired by the shape of supercritical airfoils. It provides lift, which is the most important advantage of the blended wing body configuration. This modified body has an elliptical shape for the cargo compartment and loading considerations. The middle part of the body has enough height and length for the cargo compartment. Part of the rear bottom of the body can be opened as the ramp for loading and unloading. The shape of the rear portion of the body still provides enough clearance for loading and unloading.

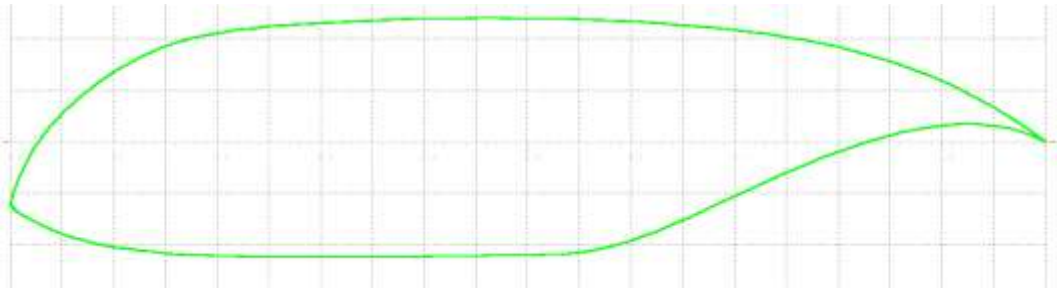

Figure 20: Shape of the Body

The lift coefficient vs. angle of attack and the drag coefficient vs. angles of attack of the body airfoil are shown in Figures 21. The lift-to-drag ratio vs. angles of attack is shown in Figure 22 below as well. These plots were generated using the software XFLR5. Because of the shape of the fuselage the aircraft will not fly above nine degrees angle of attack. Above this point, the aircraft starts to lose lift.

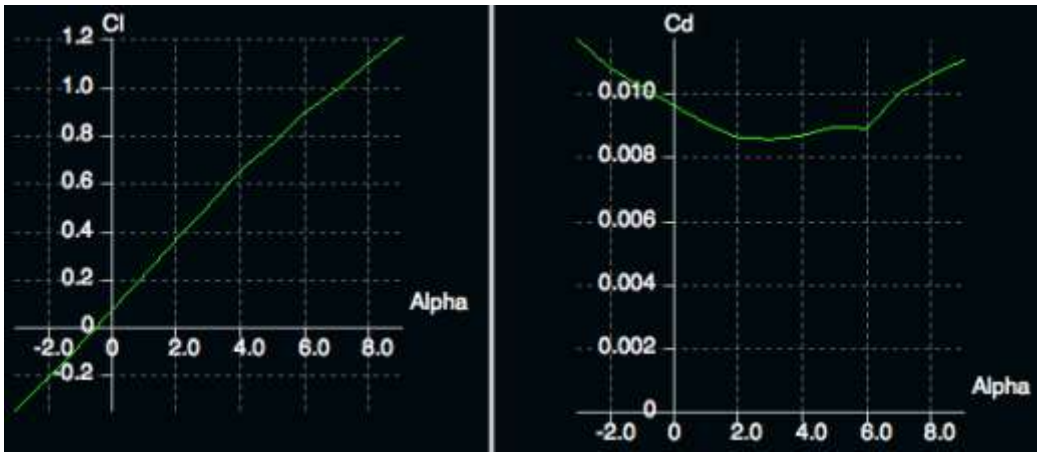

Figure 21: Lift Coefficient and Drag Coefficient vs. Angles of Attack of Body

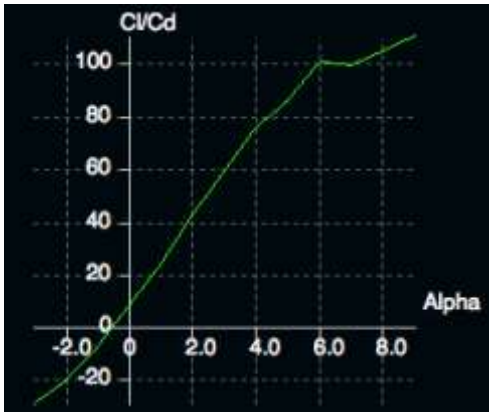

Figure 22: Lift-to-Drag Ratio vs. Angles of Attack of Body

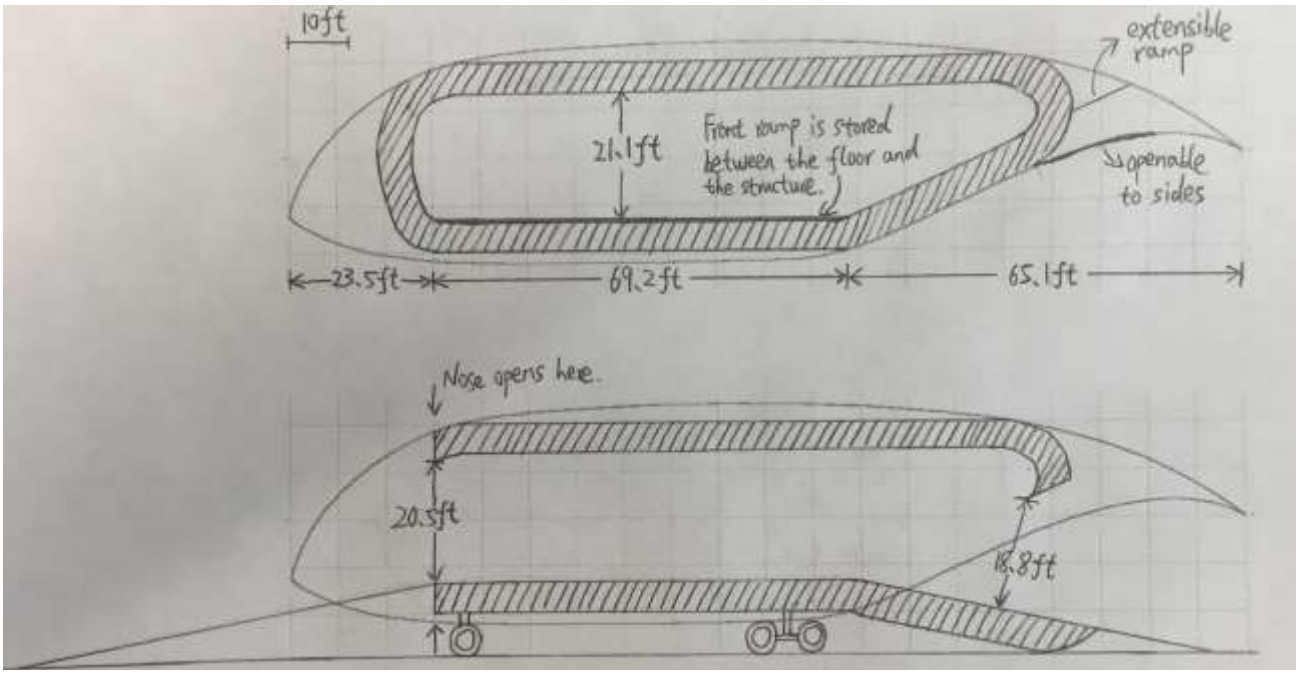

Figure 23: Sketch of Side View of Cargo Compartment with Structure Highlighted

3.10 Fuel System

The fuel weight has been calculated along with the MTOW. With that information, it is possible to calculate the necessary fuel volume, and thus the dimensions of the fuel tanks.

Taking the fuel weight fraction calculated in the resized weight estimation

$$\frac{W_f}{W_0} = 0.3349 \tag{16}$$

and knowing the resized MTOW

$$W_0 = 950000\ lb \tag{17}$$

the fuel weight will be

$$W_f = \left(\frac{W_f}{W_0}\right) * W_0 = 318155\ lb. \tag{18}$$

Taking the value of the density of the fuel as

$$\rho = 6.7 \frac{lb}{gal} \tag{19}$$

the volume can be calculated as

$$V = \frac{W_f}{\rho} = 47{,}486\ gal\ =\ 6{,}348\ ft^3. \quad (20)$$

The main fuel tanks will be in the wings. The largest percentage of fuel will be placed in the blended section of the wing.

One of the most important characteristics of the fuel system is the nitrogen injection system used for safety. While the aircraft is burning fuel, nitrogen will be injected in the fuel tank avoiding the possibility of having oxygen combust with the fuel inside the fuel tank.

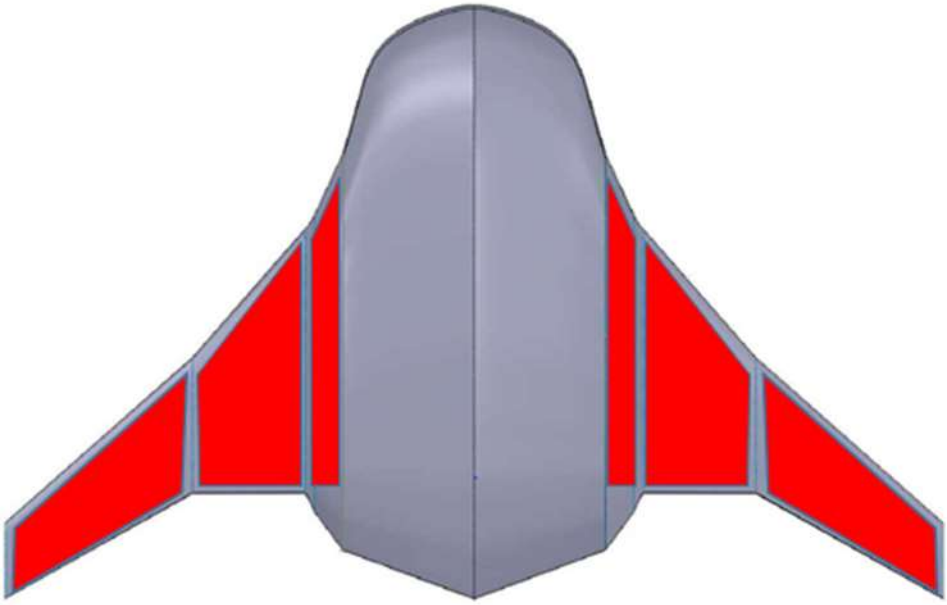

Figure 24: Fuel Location in Aircraft

Fuel tanks:

$$V_1 = S_1 * h_1 = 1{,}400 * 2.8 = 3{,}920\ ft^3$$
$$V_2 = S_2 * h_2 = 1{,}590 * 5.4 = 8{,}586\ ft^3$$
$$V_3 = S_3 * h_3 = 875 * 20 = 17{,}500\ ft^3$$
$$V_t = (V_1 + V_2 + V_3) * 2 = 60{,}012\ ft^3$$

The calculations shows that there is enough space for mission fuel of this aircraft. The fuel tanks in the blended body section will be emptied first. The wing fuel tanks are used next.

3.11 Structures

Research:
The blended wing body (BWB) concept is completely unique. Since the BWB's body is not cylindrical, developing a central body configuration to pressurize the fuselage is challenging.

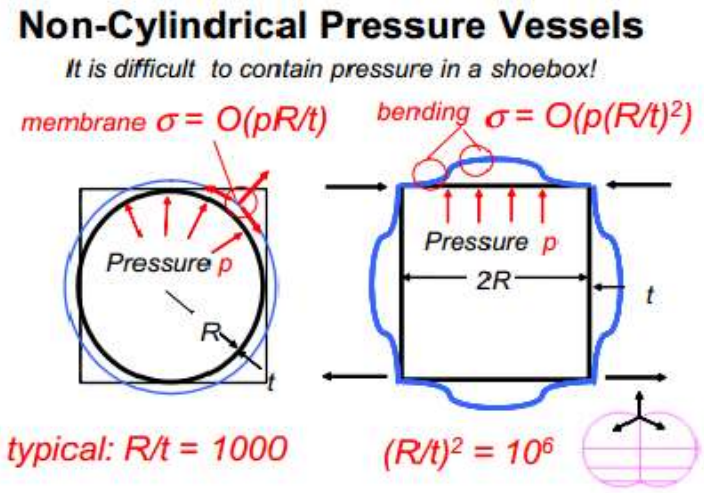

Figure 25: Internal Pressure Comparison

Figure 25 expresses that the bending stress in a square is one order of magnitude higher than that in a cylindrical section. The stress becomes primarily bending stress instead of membrane stress. V. Mukhopadhyay from NASA Langley Research Center conducted a study in which he tested how stress acted on the members of many different combinations of fuselage structure configurations.[13]

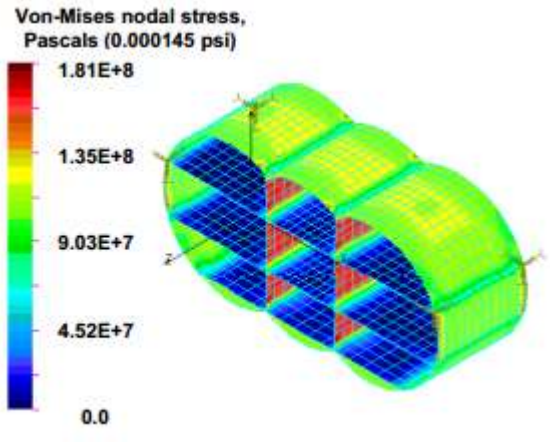

The triple bubble design seen to the left seems the best to manipulate for the AIAA competition BWB's design. With its 3-floor concept and additional outer stiffened double panels at top and bottom of the fuselage, stress was manageable in the vertical support members. This option was ideal due to its acceptable stress handling, shape, and ability to be stiffened with ring stiffeners, which are typical for transport aircraft.

Figure 26: Triple Bubble Configuration

Initial Fuselage Concept:

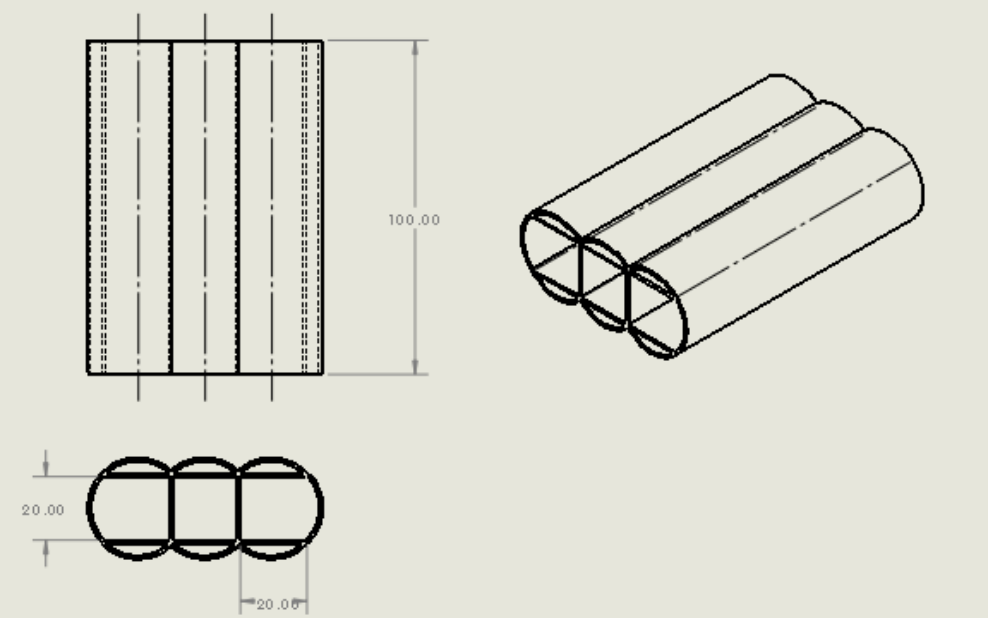

Figure 27: BWB Internal Structure (units in ft)

While the triple bubble configuration was chosen as a guide for the internal structure configuration, changes were made to suit the payload arrangement and simultaneous loading and unloading requirements. As shown in Figure 27 there are three main compartments, 20 ft by 20 ft, which is an acceptable height and width for the required payload. In comparison to the original triple-bubble design presented by V. Mukhopadhyay, this design reduces the amount of floors from three to one. Though thick aluminum is not used in aircraft, to get an idea of stresses in the fuselage caused by pressurization, the horizontal plates were set at 1''.

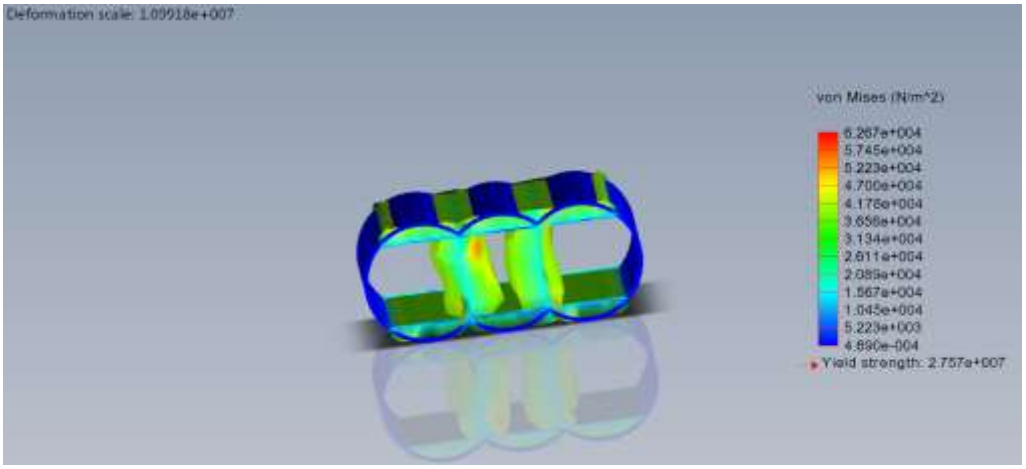

Figure 28: Stress in Initial Fuselage Concept

Figure 28 shows the stress within the fuselage caused by an internal pressure of 10.9 psi. It is common practice for military cargo planes to transport soldiers with cargo. Therefore, to avoid concerns about hypoxia, decompression sickness, and altitude sickness, an internal pressure of 10.9 psi has been chosen according to Federal Aviation Administration practices. The deformation scale in the figure above is displayed at a magnitude of 110 million in order to exaggerate what is happening in the members. The outer surface was fixed in this analysis, assuming that the surrounding supporting braces and ribs along the member would provide additional needed support. The highest stress within the member is about 6.257e +004, which is manageable for the current thickness setting of this member.

Updated Fuselage Concept:

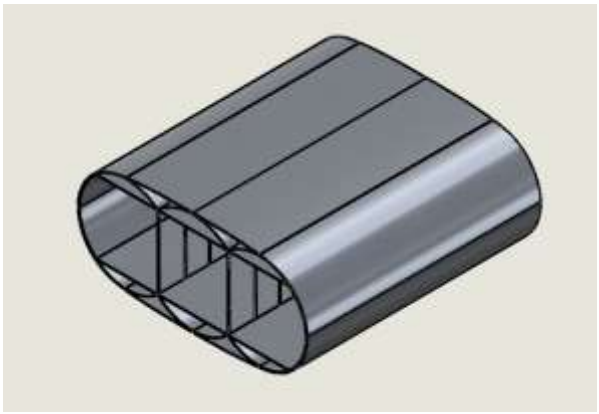

Figure 29: Updated Fuselage (View 1)

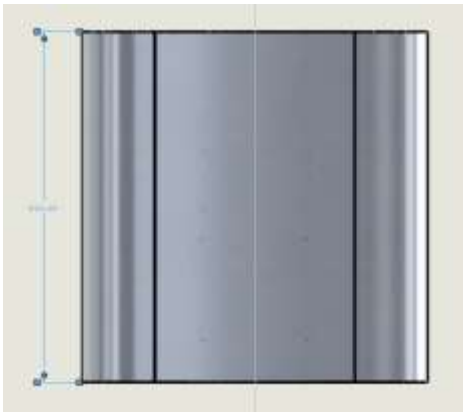

Figure 30: Updated Fuselage (Top View)

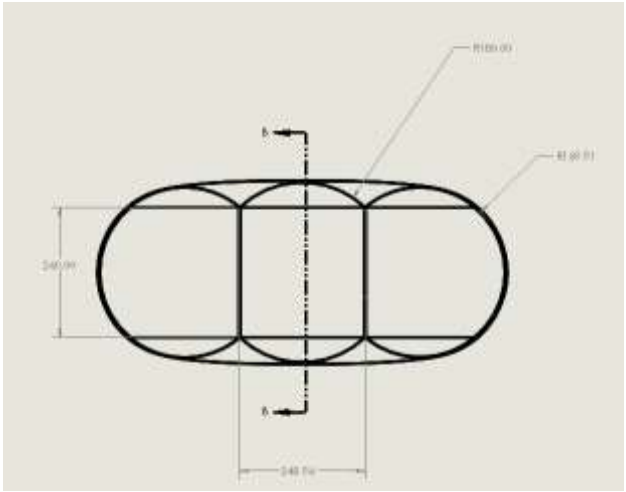

Figure 31: Updated Fuselage (Front View)

Dimensions of the internal compartment have been updated. As shown in Figures 29-31 the length has been updated to 69.2 ft, the internal height between horizontal plates is now 21.4 ft. The thicknesses of each horizontal plate and the sheets of metal forming the bubble structure is now

0.087 inches. In comparison to the old concept, the vertical plates have been replaced with tension bars, for weight reduction. Also, there is now an aluminum shell on the outer surface of the bubble structure as shown in the front view of the structure. This helps in bending and buckling spanwise not considered in the initial analysis. There are I-beams supporting the shell structure that run spanwise between the shell and bubble structure at critical points where the shell would naturally touch the bubble structure. Adjustments will be made in the future to accommodate analysis of the internal fuselage's current thickness settings.

3.12 Engine Choice and Analysis

Engine Quantity:
First and foremost for engine choice, the total number of engines is paramount in considering what types of engines to utilize for the aircraft. Using a figure of merit and fundamental statistics analysis, a total of four engines was chosen to be mounted onto the aircraft. Below is the figure of merit.

Table 13: Figure of Merit for Engine Quantity

Engine Number (1-5)	2	3	4	5
Stability (Worst Case) (1)	3	1	3	1
Aerodynamic Efficiency (1)	1	1	2	2
Controls (1)	2	2	3	3
Power Distribution (1)	1	1	2	2
Sum	7	5	10	8

The reasoning behind why four engines is statistically better/safer is because of an in-depth analysis of one of AIAA's competition mission requirements. Specifically, "the aircraft shall be able to perform a take-off, climb to pattern altitude, conduct pattern flight, and return to base with one or more engines out immediately after decision speed. Aircraft with an even number N of engines shall meet this requirement with any N/2 engine inoperative; if N is odd then assume N/2 + 1 engines inoperative…" The logic behind choosing four engines is found when calculating towards the worst case scenario. Clearly for odd numbers of engines, the total number of inoperative engines is rounded up. This means that they are out of the question. Losing more than 50% (in most cases significantly more) of the thrust available would cause an unacceptable reduction to the aircraft's performance. This cuts down the choices for engine numbers to only two engines and four engines.

For two engines, there is only two scenarios for engine inoperability: the left engine being out and the right engine being out. In both cases, they are equally affecting the aircraft's moment. For four engines, there are six scenarios that are displayed in the figure below.

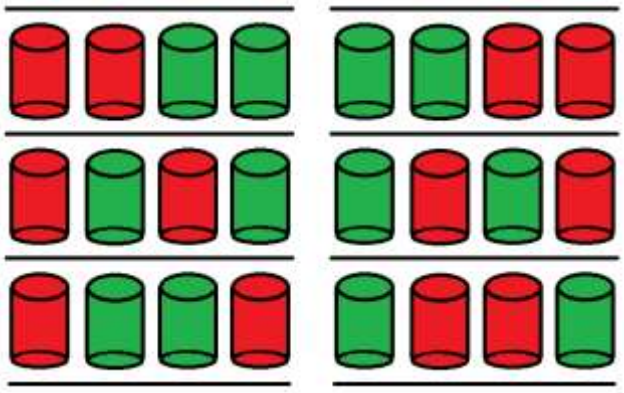

Figure 32: Four Engine Scenarios

In the two scenarios at the top of the figure, there is the most instability due to the engine inoperability. Following that is the middle row with a relatively lower level of instability but still adding to the instability of the aircraft. Finally, the bottom row displays a stable configuration even with the correct number of inoperable engines out. From this a conclusion may be made about the percentages over time of instability within the aircraft. Thirty-three percent of the time (with the given condition of N/2 engines being inoperative), the aircraft will be stable against a sixty-seven percentage for the time the aircraft is unstable. This compares favorably to the two engine option, which is always unstable in these conditions. The logical conclusion is that the aircraft should have four engines.

Engine Sizing:
The size and type of the power plants to be used for this airplane can be determined by the design thrust-to-weight ratio (in this case the take-off thrust-to-weight ratio) and the maximum take-off weight (MTOW) of the aircraft.

The aircraft is designed to be powered by four high-bypass (HBP) turbofan engines. HBP turbofan engines were selected because they are adequate for the flight conditions the airplane is expected to experience. HBP has lower TSFC which is critical for transport mission. These engines excel at flight speeds that range from 0.6 M to 0.9 M, adding to the fact that their performance is optimal at altitudes close to the expected cruise altitude of this aircraft.

Figure 33 was taken from 'Aircraft Design: a Conceptual Approach', it shows the typical performance envelope for different types of propulsion systems.[15]

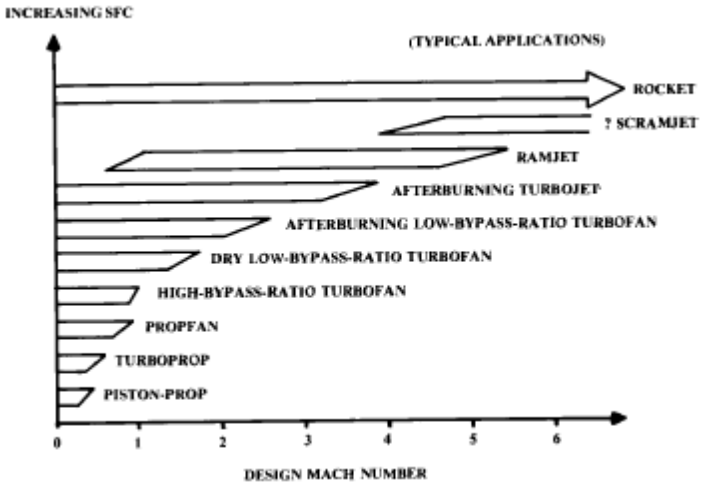

Figure 33: Typical Application for Different Propulsion Systems

To satisfy the design thrust-to-weight ratio of 0.23 and a MTOW of 950,000 lb, one power plant of 55,000 lb must be selected in order to satisfy the 220,000 lb total thrust required.

Engine Selection:
To find a power plant that suits the thrust requirements three engines from three of the largest engine manufacturers in the market were considered: General Electric CF6-80C, Pratt & Whitney JT9D-7R, and Rolls-Royce RB211.

General Specifications:
The general specifications for the engines were obtained from a jet engine catalogue.

General Electric CF6-80C
- Airplanes: Boeing 747-300
- Static Thrust: 56,700 lb
- TSFC: 0.323
- Weight: 9388 lb
- Length: 7.75 ft
- Fan Diameter: 13.3 ft

Pratt & Whitney JT9D-7R
- Airplanes: Airbus A-300
- Static Thrust: 56,000 lb
- TSFC: 0.364
- Weight: 8885 lb
- Length: 7.78 ft
- Fan Diameter: 12.8 ft

Rolls-Royce RB211
- Airplanes: Boeing 767
- Static Thrust: 56,400 lb
- TSFC: 0.330
- Weight: 9671 lb
- Length: 7.19 ft
- Fan Diameter: 10.41 ft

A figure of merit was developed to determine the engine that would be the best fir for the performance requirements of the transport aircraft. For the merit analysis, three aspects where considered: TSFC, which was weighted with three points, thrust of the engine in comparison with the thrust required by the design, scaled with two points, and weight, scored with one point. Each engine was given a rank, 3 being the highest and 1 the lowest, and a total weighted score was calculated.

Table 14: Figure of Merit for Engine Selection

	TSFC (3)	Score	Thrust (2)	Score	Weight (1)	Score	Total
GE CF6-80C	3	9	1	2	2	2	13
PW JT9D	1	3	3	6	3	3	12
RR RB211	2	6	2	4	1	1	11

The GE CF6-80C obtain the highest weighted value, thus, all the thrust and power performance calculations will be based on the values provided by this power plant.

The GE CF6 family entered service in the mid 70's. Even though it is quite an old engine, it was selected for this design with the purpose of using its data as a good estimate for the aircraft's performance. General Electric plans to replace this engine family with the GEnX family, which it is under development.

Since this airplane would enter service on 2030, the next step in the design process is to further investigate the specs of the new GEnX engines, or the Ultra-fan geared engines being developed by companies like Rolls-Royce and Pratt & Whitney.

Thrust Available:
Based on the selected engines the thrust available at sea level is 218,500 lb.

An adequate approximation for the thrust available at altitude can be obtained by multiplying the sea level thrust available (T_{sl}) by the density ratio (σ) for each altitude.

$$T_A = \sigma * T_{sl} \tag{21}$$

Thrust Required for SLUF:
For straight, level, unaccelerated flight, the thrust required can be obtained by calculating the drag generated by the airplane at given altitude and flight speed. The drag coefficient was calculated using the drag polar equation

$$C_D = C_{D_0} + C_{D_i} \tag{22}$$
$$where\ C_{D_i} = \frac{C_l^2}{\pi * e * AR}$$

thus, yielding a thrust required (T_R) of

$$T_R = C_D * \frac{1}{2} * \rho * v^2 * S\ \ [lb] \tag{23}$$

The results can be seen in the Figure 34, where they are plotted versus flight speed and altitude.

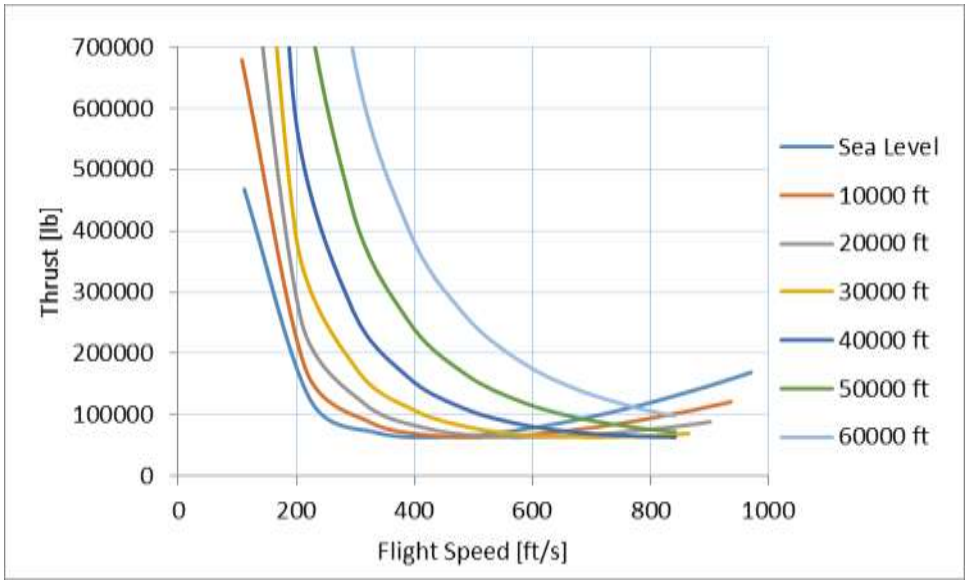

Figure 34: Thrust Required as a Function of Flight Speed and Altitude

It is of special interest to analyze the cruise conditions for the airplane since cruising is the main requirement.

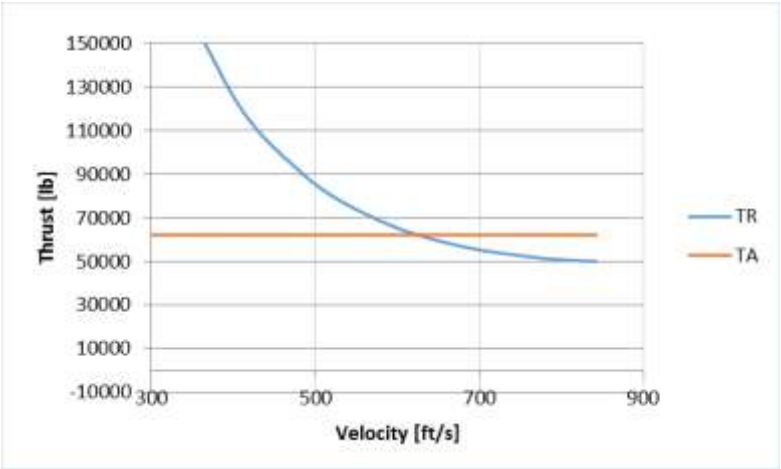

Figure 35: Thrust Required Versus Thrust Available at 36,000 ft

Power Available/Power Required:
Similarly, the power characteristics at certain flight conditions can be estimated. Power can be calculated as

$$P_i = T_i * V \tag{24}$$

where P is the resultant power, T is the thrust used or required, and V is the flight speed at which it is desired to perform flight.
To further analyze power requirements, they were plotted in a graph as a function of flight speed and altitude.

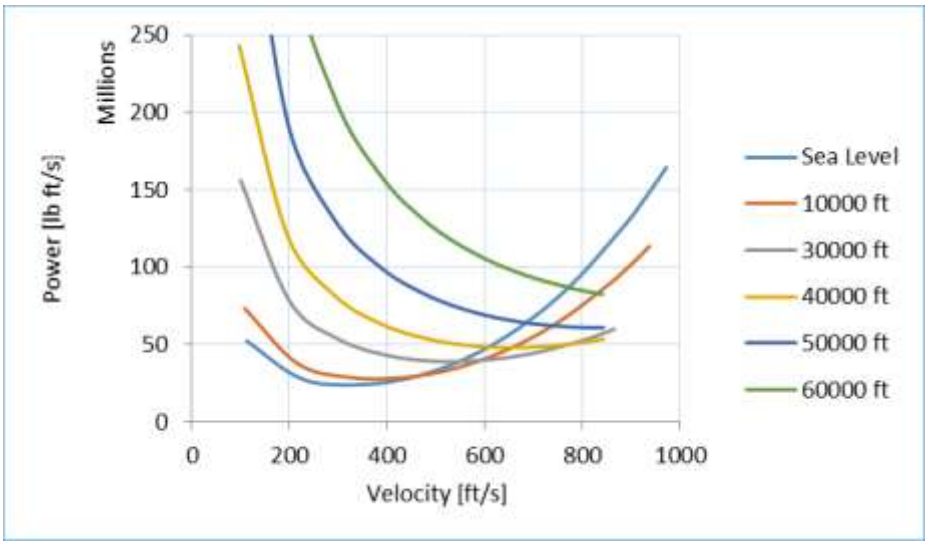

Figure 36: Power Required

The power setting was analyze in great detail for cruise conditions, the results yield

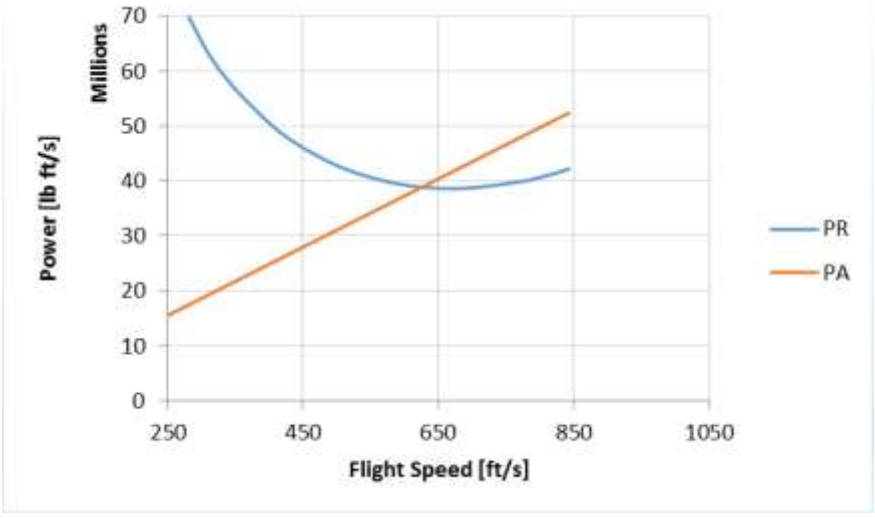

Figure 37: Power Required Versus Power Available

The analysis of both thrust and power requirements holds evidence that the power plants selected are appropriate for the transport aircraft configuration. It is clear that, for cruise conditions (36,000 ft altitude, and 0.8 M speed), the engines have enough power to sustain the required performance.

Rate of Climb:
From the power calculations, the rate-of-climb can be determined as follows

$$RoC = \frac{(P_A - P_R)}{W} \tag{25}$$

where P_A is the power available at a given altitude, P_R is the power required at the same altitude, and W is the weight of the airplane. If the maximum rate-of-climb needs to be calculated then the maximum excess power has to be used in the equation.

$$RoC_{max} = \frac{(P_A - P_R)_{max}}{W} \tag{26}$$

Calculating the rate-of-climb for each altitude can be beneficial in order to determine the time it will take the airplane to reach cruise altitude, as well as to calculate the service ceiling, and the absolute ceiling.

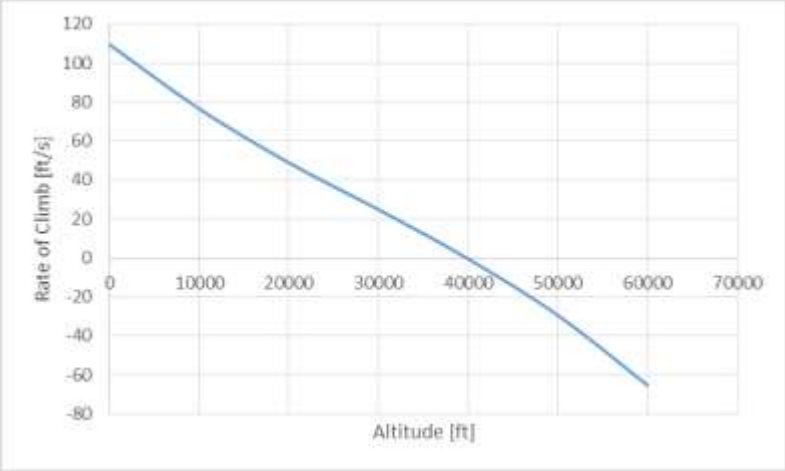

Figure 38: Rate of Climb

Under the definition provided by Raymer, the military service ceiling is that altitude at which the rate-of-climb has a value of 1.667 ft/s.[15] The absolute ceiling, on the other hand, is that altitude at which the excess power is 0.

From the plot, the service ceiling is estimated to be 39,270 ft and the absolute ceiling 39,820 ft. This results hold evidence that the designed aircraft will be able to perform at the desired cruise altitude with enough excess power to perform further climb if needed.

3.13 Weight/Moment Balance

After calculating the weight, wing loading, and thrust-to-weight ratio, the next important step is determining the center of gravity (c.g.) of the aircraft. Taking an approximate position from the nose of the aircraft, *x*, along with an estimated weight for all the elements in the aircraft, it is possible to estimate the c.g. position. The estimated weight fractions of empty weight and maximum take-off weight are based on statistics from Raymer and Nicolai.

By using a sketch and a basic Excel calculation, the following weight balance was obtained.

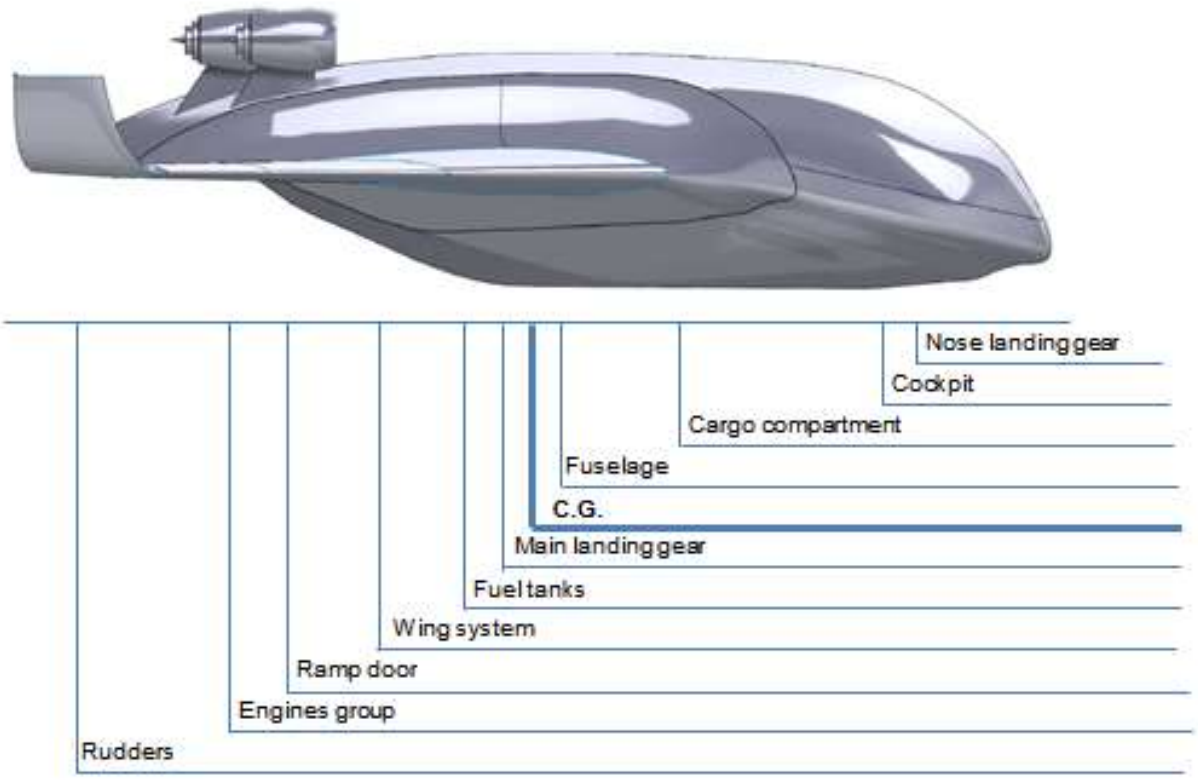

Figure 39: Weight Balance

The wing system of the aircraft were placed aft of where the middle of the aircraft would be. This is because they are needed to offset the enormous weight of the cargo which has a c.g. forward of the middle of the aircraft. Along with the four engines and control surfaces, the c.g. ends up being behind the middle point of the aircraft. This weight compensates for the cargo compartment, fuselage, and the systems placed in front of the middle of the aircraft.

After all the calculations, the total moment was generated for all the elements of the aircraft and summed. This moment should be equal to the moment created by the total weight of the aircraft at the c.g. position.

$$\sum x_i * W_i = x_{cg} * W_e \tag{27}$$

(See the appendix for the Excel sheet)
Finally, the c.g. position was calculated to be 77.92 ft from the nose of the aircraft.

3.14 Mean Aerodynamic Chord

Mean Aerodynamic Chord:
Using the previously calculated wing surface of S = 14,400 ft^2 and an aspect ratio of approximately 4, as well as taking into account that the surface of the body is also part of the wing surface, a mean aerodynamic chord, MAC, may be determined. Due to the shape of the design, the body also provides lift.

When attempting to determine a common wing configuration for a blended wing body aircraft, the following design was chosen.

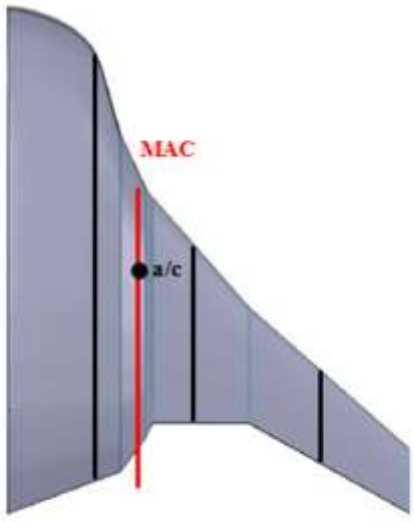

Figure 40: Wing Configuration and MAC

Figure 40, the aerodynamic center is drawn, which is placed at the quarter point of the aerodynamic chord. The mean aerodynamic chord was calculated by dividing the wing and body into three trapezoidal parts.

The MAC calculations are:

$$MAC = \frac{mac_1 * S_1 + mac_2 * S_2 + mac_3 * S_3}{S_1 + S_2 + S_3} = 94.19\ ft \quad (28)$$

$$d = \frac{d_1 * S_1 + d_2 * S_2 + d_3 * S_3}{S_1 + S_2 + S_3} = 41.09\ ft \quad (29)$$

$$m = \frac{m_1 * S_1 + m_2 * S_2 + m_3 * S_3}{S_1 + S_2 + S_3} = 56.26\ ft \quad (30)$$

Table 15: MAC Calculations

MAC - 3 Different Part			
mac_1	28.76 ft	S_1	1400.00 ft^2
mac_2	54.82 ft	S_2	1590.00 ft^2
mac_3	133.28 ft	S_3	3945.00 ft^2
mac_{Total}	94.19 ft	S_{Total}	6935.00 ft^2
mac_{Wing}	42.62 ft		
$mac_{Fuselage}$	133.28 ft		
d_1	103.50 ft	m_1	133.30 ft
d_2	55.00 ft	m_2	85.00 ft
d_3	13.33 ft	m_3	17.33 ft
d_{wing}	77.71 ft	m_{wing}	107.62 ft
d	41.09 ft	m	56.26 ft
$d_{fuselage}$	13.33 ft	$m_{fuselage}$	17.33 ft
a/c f	50.65 ft		
a/c w	118.27 ft		

The position of the aerodynamic center with respect to the c.g. of the aircraft has to be between a set interval of values to assure that the aircraft is statically stable, with positive static margin < 0.1.

This aircraft is statically stable:

Table 16: Static Stability Calculations

Static Stability		
a/c	79.80	ft
x_{cg}	77.92	ft
Static margin	0.02	2%
x_a/MAC	0.85	
Static margin	0.10	10%
x_{cg}/MAC	0.75	max forward
x_{cg} max forward	70.38	ft

3.15 Control Surfaces

Basic calculations for the control surfaces were made based on research data from blended wing body and military cargo aircraft.

New detailed calculations will be performed with the stability requirements, which will provide a more accurate set of data for the control surfaces.

The aircraft will have four vertical tails: two close to the center of the fuselage and two placed on the wing tips. Elevons are placed on the body and wings. Ailerons are as shown in the Figure 41.

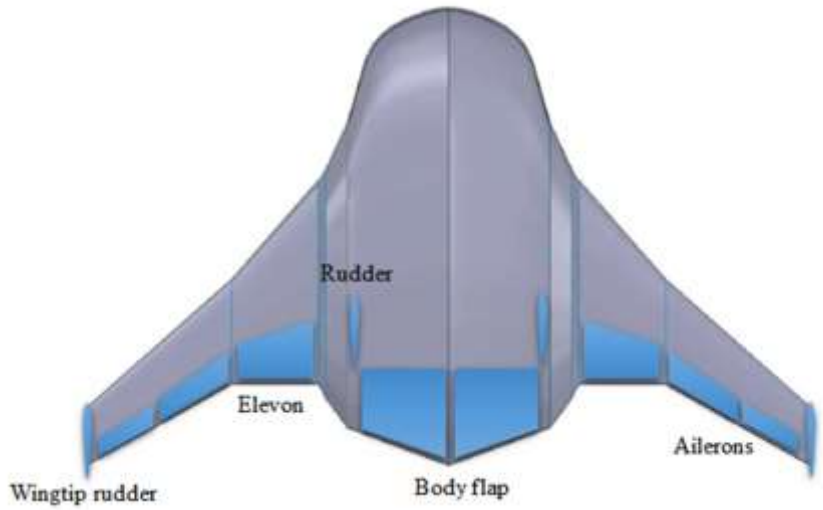

Figure 41: Diagram of Control Surfaces

$$S_r = \frac{c_r * S_w * b_w}{l_r} \tag{31}$$

$$S_e = \frac{c_e * S_w * c_w}{l_e} \tag{32}$$

Estimated values		
V Tail volume coefficient (table)	0.08	
H Tail volume coefficient (table)	0.95	
Rudders in the center	1227.83	ft^2
Rudder in wingtips	851.27	ft^2
Body flap	3700.34	ft^2
Elevons	3700.34	ft^2
Ailerons	1400.00	ft^2

Figure 42: Control Surface Calculations

3.16 Landing Gear

The landing gear of the aircraft is determined mainly from its c.g. and weight. With a weight of approximately 950,000 lb, an aft c.g. of 80 ft, and a forward c.g. of 75 ft, the locations of the nose and main landing gears may be obtained. Using a method explained in Currey, the nose landing gear position was determined to be at 12.5 ft from the nose of the aircraft.[6] The main landing gear was determined in a similar method and found to lie at 87 ft from the nose of the aircraft. Using this configuration, the nose landing gear will be holding approximately 8% of the total weight of the aircraft, with the remaining weight being distributed on the main landing gear.

Looking at historical data for the C5-A, the An-225, and other cargo aircrafts, a tire size of 49 x 17 was arbitrarily decided on. Because of the design of the aircraft, the wheel configuration will be in a two twin delta in tandem formation, TTDT. For the main landing gear, with 92% of the aircraft weight being distributed on *x* number of 49 x 17 tires, the optimal amount of wheels is thirty. These wheels will be dispersed in sets of six on five different struts. Two struts on the left and right side of the fuselage along with two sets of three wheels in a delta formation heading each side. The nose landing gear will consist of simply four wheels side by side.

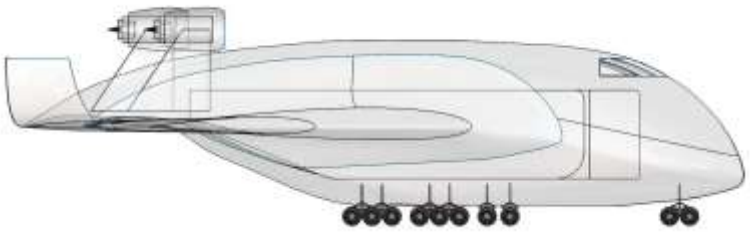

Figure 43: Side View of Landing Gear

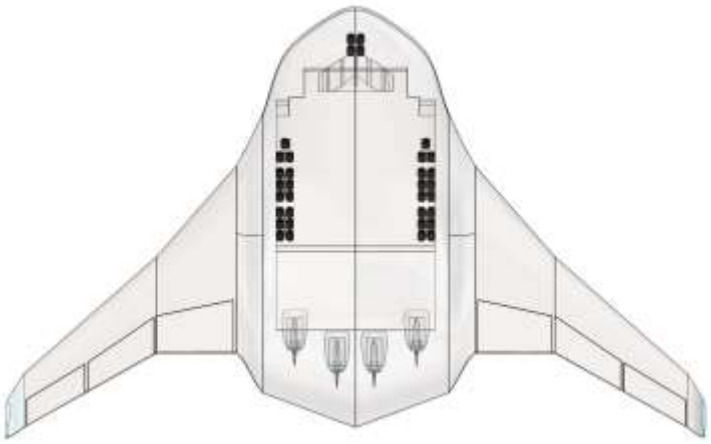

Figure 44: Bottom View of Landing Gear

The placement of the landing gear was determined in consideration of where the fuel tanks are to avoid accidental explosion upon high impact landings. The landing gear will be fixed to their positions on the aircraft. They will have the ability to move outward into a more aerodynamic position, but because of the cargo compartment requirements, there is no space for the landing gear to be retractable.

3.17 Performance

3.17.1 Take-off

Due to the unusual configuration of the blended wing body aircraft, the statistical methods normally used to calculate control surfaces are invalid.

To obtain the correct values and results necessary, analysis of extreme situations where control surfaces is needed i.e. take-off or landing.

One of the most important conditions is take-off. Because of the configuration of the aircraft, the lift created form the wings are going to generate the contrary pitch moment needed for take-off. On the other hand, the lift created form the center body section generates the pitch moment that the aircraft needs to achieve.

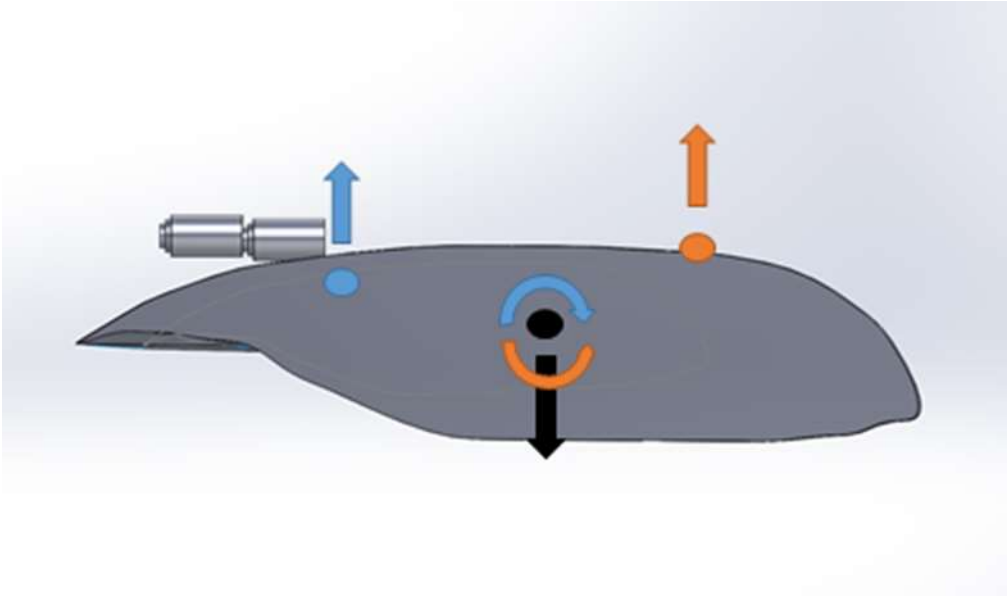

Figure 45: Pitch Moments Diagram

Using the average method for take-off distance, it can be shown that with a body flap of 1000 ft^2, and elevens of 1000 ft^2, the aircraft generates a positive pitch moment and can take-off within the necessary distance of 9,000 ft.

Table 17: Take-off Stability Calculations

Take-off calculations											
Fuselage				Wing				Total			
	Cl alpha	0.15	1/degree		Cl alpha w	0.11	1/degree		S	14400.00	ft^2
	CL alpha	0.96	1/degree		CL alpha w	4.20	1/degree		CL max	1.45	
	AR	0.34			AR	4.00			W	950000.00	lbf
	b	60.00	ft		b	240.00	ft		ro SL	0.00	$slug/ft^3$
	S	10480.00	ft^2		S	3920.00	ft^2		V LOF	236.58	ft/s
	L	6954.08	lbf		L	1907.50	lbf		V STALL	215.08	ft/s
	Pitch M	**189637.65**	**lbf*ft**		**Pitch M**	**-76977.36**	**lbf*ft**		cg	77.92	ft
	lf	27.27	ft		lw	-40.36	ft		a/c	79.88	ft
	a/c f	50.65	ft		a/c w	118.28	ft		alpha	0.04	rad
	Cl max f	1.20			Cl max w	1.20			Cl max	1.20	
	CL max f	1.06			CL max w	10.62					
	Cl max b	1.08			Cl max e	1.08					
	CL max t	3.34			CL max t	10.62					
	delta b	0.26	rad		delta e	0.17	rad				
	cl max	2.28			delta a	0.17	rad				

Table 18: Take-off Calculations (Cont.)

Cl opt	0.134	
K	0.094	
Cd0	0.008	
Cd avg	0.010	
q sl	27.499	
p sl	0.002	slug/ft^3
g	32.200	ft
S	16400.000	ft^2
Davg	3987.223	lbf
W	950000.000	lbf
Lavg	52871.818	lbf
Tavg	236000.000	lbf
Vstall	195.468	ft/s
Vlof	215.015	ft/s
Vg avg	152.016	ft/s
CL max	1.451	
Sg	3253.985	ft
a	7.104	ft/s^2

3.17.2 Flight Mechanics

Drag:

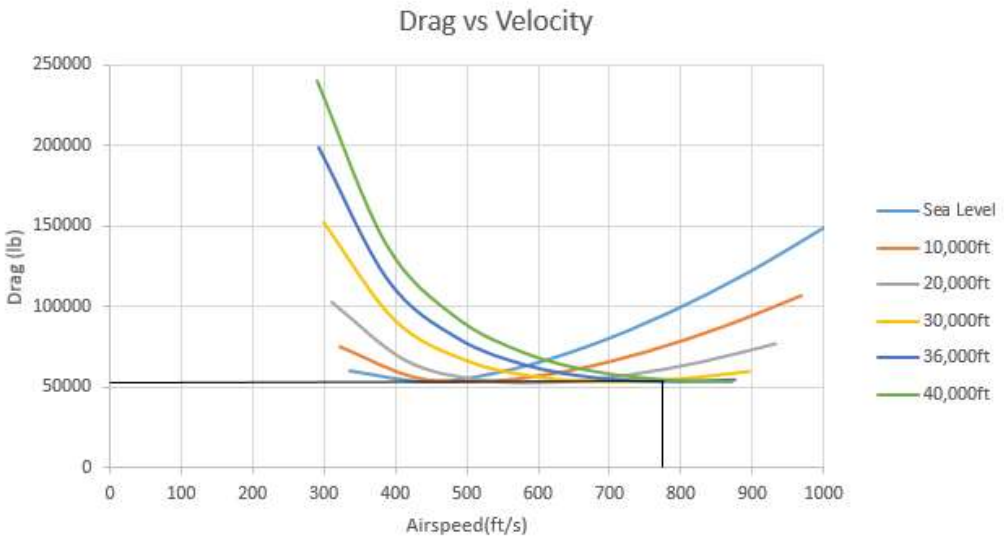

Figure 46: Drag Profile at Different Altitudes

From the graph it can be observed that parasite drag is extremely dominant over induced drag in the entire subsonic region. By analyzing the graph, it can be shown that the optimal altitude for a cruise speed is 0.8 Mach is 36,000 ft.

At the cruise altitude of 36,000 ft, the aircraft stalls at a true airspeed of 307 ft/s. L/D max occurs at minimum drag which occurs at 870 ft/s (or 0.9 Mach) with values of 17.8 and 53000 lbs respectively. These value were derived using the following equations:

$$D = C_D Q S \tag{33}$$

Where: $C_D = C_{d_0} + K{C_l}^2$

$Q = \frac{1}{2}\rho V^2$

$K = \frac{1}{\pi e AR}$

Stall speed is evaluated Lift = Weight and this is calculated using the following equation:

$$V_{stall} = \sqrt{\frac{2W_2}{\rho S C_{L_{max}}}} \tag{34}$$

Minimum Drag occurs when Parasite Drag equals Induced Drag and therefore:

$$D_{min} = 2C_{d_0} Q S \tag{35}$$

And

$$L/D_{max} = \frac{1}{2\sqrt{KC_{d_0}}} \tag{36}$$

Even with half the engines out, the aircraft has the ability to cruise at the desired speed and altitude.

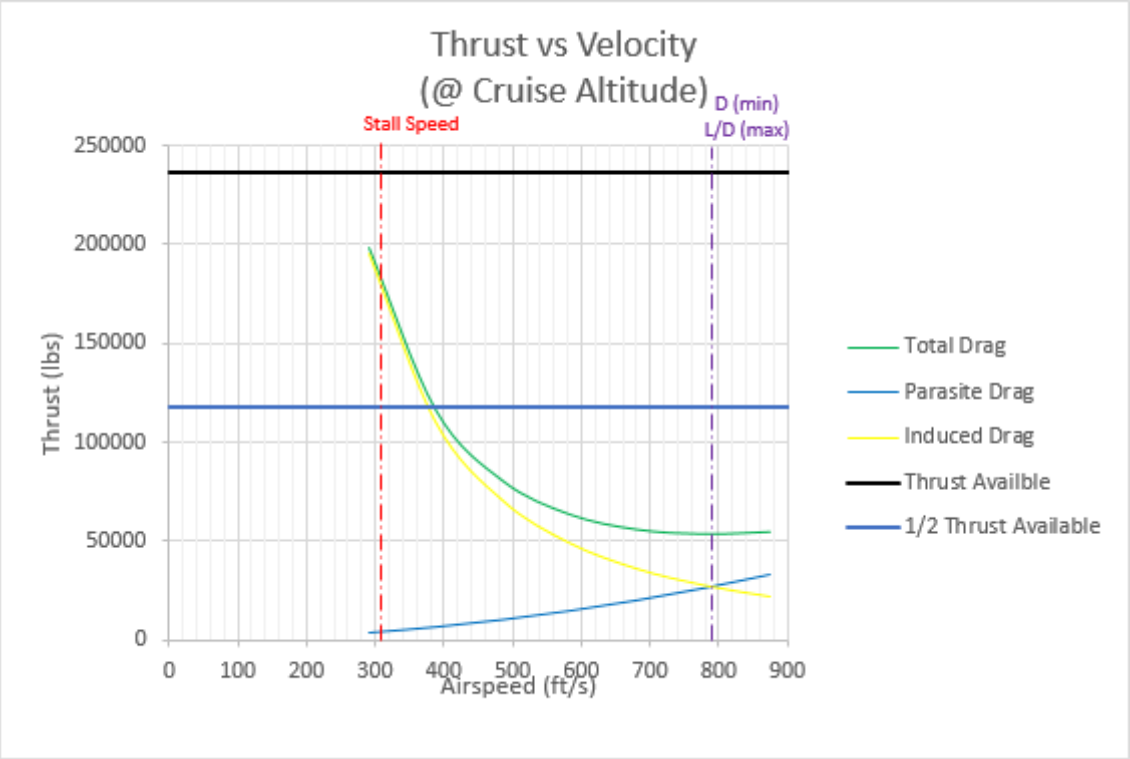

Figure 47: Thrust Versus Velocity at the Cruise Altitude

Power:

The aircraft has enough power available to take-off at desired airspeed at altitudes of up to 10,000 ft. At the half power condition, the aircraft will be required to accelerate further to a velocity of 230 ft/s in order to take-off which extends the take-off distance by 4,200 ft to 7,450 ft which is still below the required take-off distance.

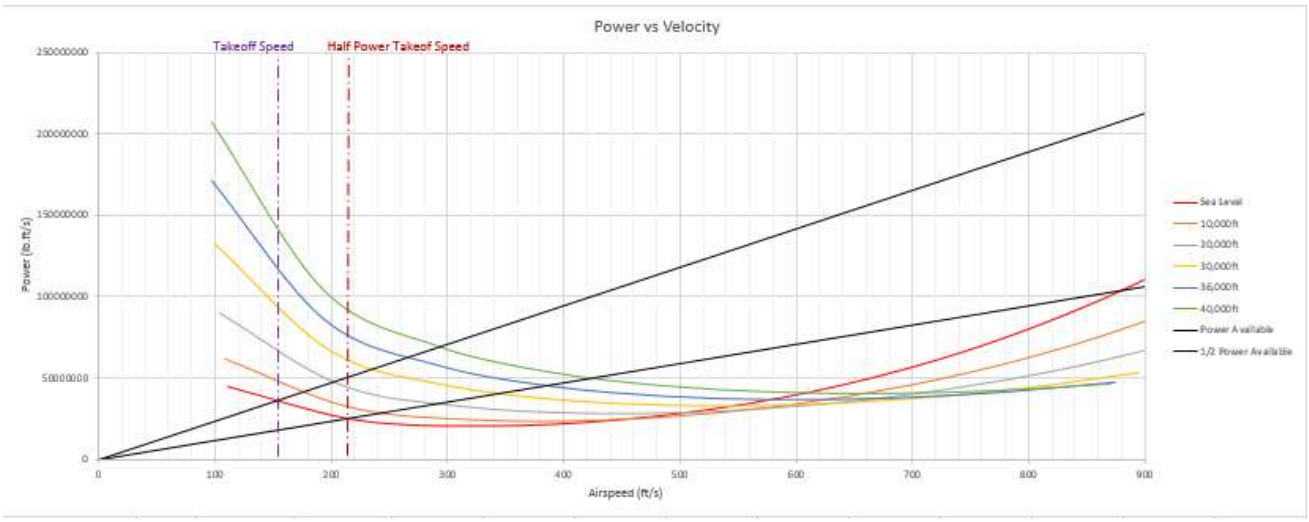

Figure 48: Power Versus Velocity

At the cruise altitude, maximum endurance can be obtained by finding the minimum power value and maximum range occurs when the gradient of the curve intercepts the origin. The value for maximum endurance is 7.47 hours at 32,000,000 lb.ft/s and 600 ft/s. Maximum range is 9,000 nautical miles at 760 ft/s.

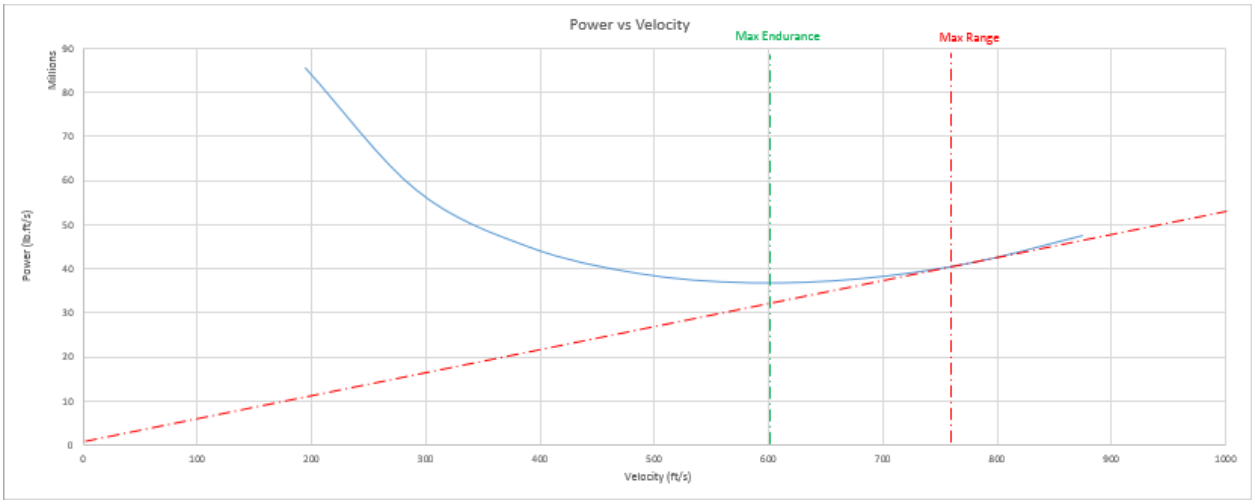

Figure 49: Power Versus Velocity (with Max Range and Endurance)

3.18 Flight Controls

3.18.1 Stability Control and Handling

Stability in a stable aircraft is, when disturbed, the aircraft tends to return by itself to its original state. “Static stability” is present if the forces created by the disturbed state push in the correct direction to return the aircraft to its original state.

Dynamic stability is present if the dynamic motions of the aircraft will eventually return the aircraft to its original state. The manner in which the aircraft returns to its original state depends on the restoring forces, mass distribution and "damping forces."

3.18.2 Longitudinal Static Stability and Control

Pitching-Moment Equation and Trim:
Pitching-moment contribution includes the wings, fuselage, body flap and elevens. In this case, the fuselage and body flap will generate a contrary contribution to the pitching moment to the wings and elevens due to the different relative position of the aerodynamic center based on the center of gravity.

For a static "trim" condition, the total pitching moment must equal zero. For static trim, the main flight conditions of concern are during the takeoff and landing with flaps and landing gear down and during flight at high transonic speeds.

Static Pitch Stability:
For static stability to be present, any change in angle of attack must generate moments which oppose the change. In other words, the derivative of pitching moment with respect to angle of attack must be negative.

The magnitude of the pitching-moment derivative changes with the c.g. location. For any aircraft there is a c.g. location that provides no change in pitching moment as angle of attack is varied. This "airplane aerodynamic center," or neutral point represents neutral stability and is the most-aft c.g. location before the aircraft becomes unstable. If the c.g. is ahead of the neutral point (positive static margin), the pitching-moment derivative is negative so the aircraft is unstable.

$$C_{m\alpha} = -C_{L\alpha}(\overline{X_{NP}} - \overline{X_{cg}}) \tag{37}$$

For the stability, the total contribution of Cm with the variation of α has to be negative. In our case, the wing is going to generate a counterclockwise pitching moment and the fuselage is going to compensate with a clockwise moment.

$$C_{m\alpha} < 0 \tag{38}$$

The results is:

$$\overline{X_{np}} = 0.24$$

That means that the more aft value of X_{cg} can be $0.24\bar{c}$, so the c.g. is going to always be more forward than the aerodynamic center of the wing. The conclusion of that is that the aircraft is stable.

And with and static margin of

$$\overline{(X_{np} - X_{cg})} = 0.02 \tag{39}$$

Contribution to Wing and Tail:
For a wing-alone design to be statically stable, tells us that the aerodynamic center must be aft of the center of gravity to make $C_m < 0$. Since we also want to be able to trim the aircraft at a positive angle of attack, the pitching moment coefficient at zero angle of attack, C_{mo}, must be greater than 0. For many airplanes, the center of gravity position is located slightly aft of the aerodynamic center. But not in this case, as it was said before, the wing pitching moment contribution is counterclockwise, the a/c of the wing is aft of the c.g.

Trim Analysis:
An airplane is said to be trimmed if the forces and moments acting on the airplane are in equilibrium. By setting the pitching moment equation equal to 0 (the definition of trim), the elevator angle required to trim the airplane may be solved for.

Getting the parameter τ from the graph:

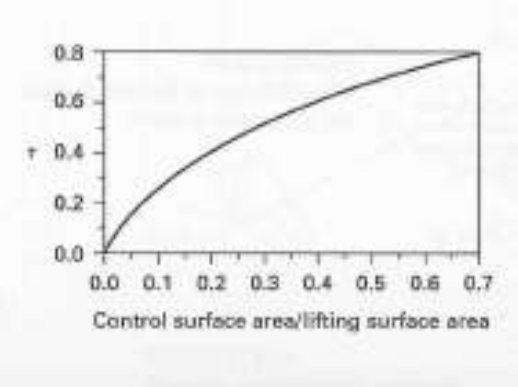

Figure 50: Trim Parameter Graph

And calculating:

$$C_{m\delta e} = C_{L\delta e} * le \tag{40}$$

$$C_{Ltrim} = \frac{W}{q*S*c} \tag{41}$$

$$\Delta C_L = C_{L\delta e} * \delta_e \tag{42}$$

$$\delta_{etrim} = \frac{C_{m0}*C_{L\alpha}+C_{m\alpha}*C_{Ltrim}}{C_{m\delta e}*C_{L\alpha}-C_{m\alpha}*C_{L\delta e}} = 0.0334 \text{ rad} \tag{43}$$

$$\alpha_{trim} = \frac{C_{Ltrim}-C_{L\delta e}*\delta_{etrim}}{C_{L\alpha}} = 0.092 \text{ rad} \tag{44}$$

Directional and Roll Stability:
Directional, or weathercock, stability is concerned with the static stability of the airplane about the z axis. Just as in the case of longitudinal static stability, it is desirable that the airplane should tend to return to an equilibrium condition when subjected to some form of yawing disturbance. To have static directional stability the slope of the yawing moment curve must be positive $C_{n_\beta} > 0$. Note that an airplane possessing static directional stability will always point into relative wind, hence the name weathercock stability.

The contribution of the wing to directional stability usually is quite small in comparison to the fuselage. And the wing-fuselage contribution is destabilizing.

The vertical tail must be properly sized to ensure that the airplane has directional stability. The coefficient moment produced by the vertical tail can be written:

$$C_n = \frac{N_{vt}}{Q_w * S * b} = \frac{l_{vt} * S_{vt} * Q_{vt}}{S * b * Q_w} * C_{L_{\alpha_{vt}}} * (\beta + \sigma) = V_{vt} * \eta_{vt} * C_{L_{\alpha_{vt}}} * (\beta + \sigma) \quad (45)$$

So:

$$Cn_{\beta_{vt}} = V_{vt} * \eta_{vt} * C_{L_{\alpha_{vt}}} * \left(1 + \frac{d\sigma}{d\beta}\right) \quad (46)$$

Directional control is achieved by a control surface called rudder, located on the vertical tails and the winglets in this specific case. By rotating the flap, the lift force (side force) on the fixed vertical surface can be varied to create a yawing moment about the center of gravity. The size of the rudder is determined by the directional control requirements. The rudder control effectiveness is the rate of change of yawing moment with rudder deflection angle:

$$C_{n_{\delta_r}} = -\eta_{vt} * V_{vt} * \frac{dC_{L_{vt}}}{d\delta_r} \quad (47)$$

Where:

$$\frac{dC_{L_{vt}}}{d\delta_r} = \frac{dC_{L_{vt}}}{d\alpha_{vt}} * \frac{d\alpha_{vt}}{d\delta_r} = C_{L_{\alpha_{vt}}} * \tau \quad (48)$$

An airplane possesses static roll stability if a restoring moment is developed when it is disturbed from a wings-level attitude. The restoring moment can be shown to be a function of the sideslip angle β. The requirement for stability is that $C_{l_\beta} < 0$. The roll moment created on an airplane when it starts to sideslip depends on the wing dihedral, wing sweep, position of the wing on the fuselage, and the vertical tail.

The contribution to dihedral effect from the vertical tail is produced by the side force on the tail due to sideslip. The side force on the vertical tail produces both a yawing moment and a rolling moment. The rolling moment occurs because the center of pressure for the vertical tail is located

above the aircraft's center of gravity. The rolling moment produced by the vertical tail tends to bring the aircraft back to a wings-level attitude.

Roll control is achieved by the differential deflection of small flaps called ailerons and the elevons. They modify the spanwise lift distribution so that a moment is created about the x axis.

$$C_l = C_{l_\alpha} * \frac{d\alpha}{d\delta_a} * \delta_a = C_{l_\alpha} * \tau * \delta_a \tag{49}$$

So:

$$C_{l_a} = \frac{2 * C_{L_{\alpha_w}} * \tau * c_r}{S * b} \int_{y_1}^{y_2} \left[1 + \left(\frac{\lambda - 1}{\frac{b}{2}}\right) * y\right] * y \, dy \tag{50}$$

With these equations and the software xfoil simulating a close model:

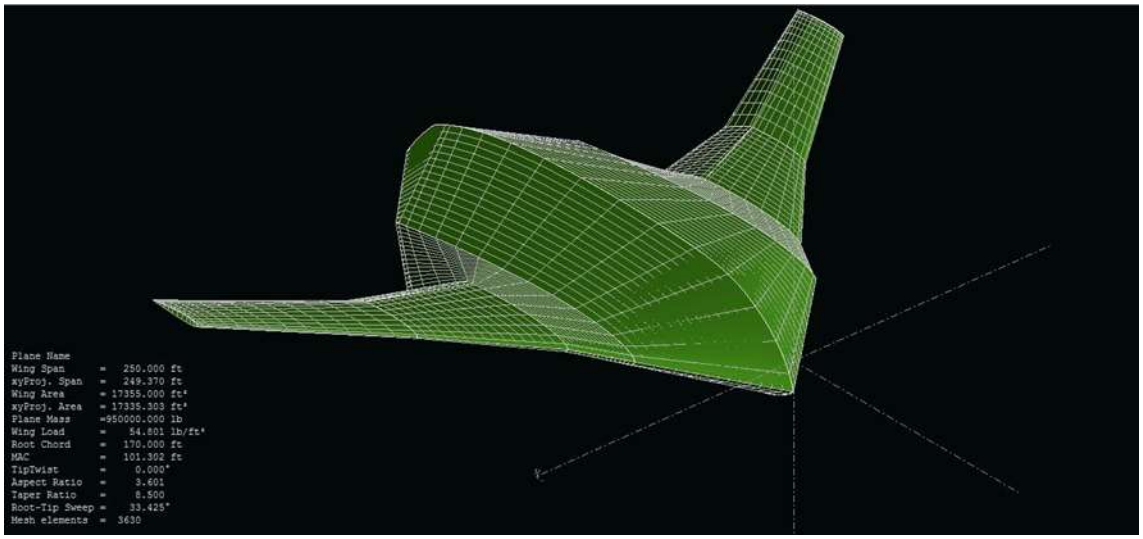

Figure 51: Xfoil Simulation

After stability and performance calculations, the obtained geometrical data and longitudinal, direction and lateral coefficients are:

Table 19: Geometric Data Set

Geometric Data		
x_{cg}	77.92	ft
x_{ac}	79.8	ft
MAC	94.19	ft
$Mach$	0.8	
W	950000	lbf

S	14400	ft^2
S_w	4920	ft^2
S_f	9480	ft^2
l_e	120	ft
$l_{bofyflap}$	150	ft
S_e	2000	ft^2
S_{vt}	3000	ft^2
l_{vt}	50	ft
b	240	ft
Γ	0.035	
λ_w	0.286	
λ_t	0.8	
$l_{winglets}$	75	ft
$S_{winglets}$	1000	ft^2
S_r	2500	ft^2
$y_{winglets}$	120	ft
y_{vt}	30	ft

Table 20: Lateral and Directional Coefficients

Stability Coefficients		
Longitudinal		
CD_0	0.008	
CL_0	0.117	
Cm_0	0.058	
CL_{max}	1.290	
CL_α	5.451	*1/rad*
Cm_α	-0.109	*1/rad*
$Cl_{bodyflap}$	2.047	*1/rad*
$Cm_{bodyflap}$	1.567	*1/rad*
$CL_{\delta e}$	3.219	*1/rad*
$Cm_{\delta e}$	-1.438	*1/rad*
δe_{trim}	0.033	*rad*
CL_{trim}	0.607	
$\left(\frac{\delta e}{CL}\right)_{trim}$	-0.015	*rad*
$Cz_{\delta e}$	-1.129	*1/rad*
Cx_α	0.004	*1/rad*
Cz_α	-5.459	*1/rad*
Cm_q	0	

Cz_q	0	
$Cz_{\dot{\alpha}}$	0	
$Cm_{\dot{\alpha}}$	0	
Cz_u	-0.442	
CL_u	0.208	

Table 21: Lateral and Directional Coefficients

Lateral and directional		
Cl_β	-0.1	*1/rad*
Cn_β	0.159	*1/rad*
Cy_β	-0.679	*1/rad*
$Cn_{\delta a}$	0.005	*1/rad*
$Cl_{\delta a}$	0.219	*1/rad*
$Cn_{\delta r}$	-0.09	*1/rad*
$Cl_{\delta r}$	-0.293	*1/rad*
$Cy_{\delta r}$	-0.351	*1/rad*
$CL_{\delta r}$	1.84	*1/rad*
Cl_p	-0.379	*1/rad*
Cn_p	-0.062	*1/rad*
Cy_p	0.649	*1/rad*
Cy_r	0.354	*1/rad*
Cn_r	-0.09	*1/rad*
Cl_r	0.086	*1/rad*

3.19 Cost Analysis

3.19.1 Project Cost

A preliminary cost analysis was done to estimate various costs associated with the aircraft project. The analysis includes clear identification of main cost groups. The cost analysis used to obtain the total cost was done under the assumption that aircrafts are priced mainly on a proportion to their gross weight. The model used was from the Raymer and Nicolai textbooks, namely the RAND DAPCA IV Model.[14][15] Many of the equations used were created with historical data from many different types of aircrafts and their cost estimates. Below are the equations used for each specific cost estimation.

$$E = 4.86\, W^{0.777} S^{0.894} Q^{0.163} \tag{51}$$

where E is the cumulative total airframe engineering hours, W is the empty weight in pounds, S is the maximum speed (kt) at best altitude, and Q is the cumulative quantity produced. Additionally,

the quantity produced takes into account the number of test aircrafts as well using the following relationship:

$$Q = Q_D + Q_P \tag{52}$$

where Q_D and Q_P are the test crafts and production aircrafts respectively. The engineering hours include design studies, engineering for wind tunnel models, mock-ups, engine tests, and others.

The development support cost, *D*, is all the nonrecurring manufacturing effort that is used to support the engineering in the aircraft program. This is the cost for manufacturing labor and material required to produce the mock-ups, test parts, etc. It is calculated with,

$$D = 66\, W^{0.63} S^{1.3}. \tag{53}$$

The flight test operations cost, *F*, is the cost elements that include what the aircraft builder requires to carry out the flight tests on the aircraft. This includes instrumentation, fuel and oil, and even pilot's pay. It is calculated with,

$$F = 1852\, W^{0.325} S^{0.822} Q_D^{1.21} \tag{54}$$

The tooling hours, *T*, are the hours charged for tool design, tool fabrication, production test equipment, production planning, and others. It is calculated using,

$$T = 5.99\, W^{0.777} S^{0.696} Q^{0.263}. \tag{55}$$

The manufacturing hours, *L*, are the total number of hours used to physically fabricate, process, and assemble the major structure of the aircraft. It is estimated with,

$$L = 7.37\, W^{0.82} S^{0.484} Q^{0.641}. \tag{56}$$

The quality control cost, *QC*, is the cost for the inspection of all the fabricated and purchased parts, assembled items against various forms of specifications. It is seen as a function of the manufacturing hours.

$$QC = 0.076\, L \tag{57}$$

The equation above is specifically for cargo and transport aircraft.

Finally, the manufacturing material and equipment cost, *M*, is the cost for all the materials and equipment necessary to create the aircraft. These include raw materials, raw castings, wires, cables, fasteners, pumps for fuel, valves, fixtures, and many other items. The cost for this is calculated with,

$$M = 16.39\, W^{0.921} S^{0.621} Q^{0.799}. \tag{58}$$

The last part of estimating a cost for the entire project is an estimation of the avionics and engine cost. The engine has been chosen, thus the value is already set.

The avionics cost varies depending on what functions are necessary to be completed. An estimate of $250,000 was used for each of the avionic systems cost in the current aircraft. This was done using historical data presented in the Nicolai textbook.

The total cost of the entire project including the research, development, manufacturing, and the tooling necessary is displayed in the Table 17. The total estimate comes out to approximately $48.6 billion. The bulk of the cost comes from the manufacturing cost.

Table 22: Summary of Costs by Standard Section

Developmental Support Cost	$737,135,202.54
Flight Test Operations Cost	$108,813,576.09
Manufacturing Material/Equipment Cost	$5,889,117,778.52
Production Engine Unit Cost	$23,420,400.66
Avionics Cost	$33,250,000.00
Tooling Cost	$7,359,495,538.73
Engineering Cost	$11,420,993,935.00
Quality Control Cost	$1,795,162,806.53
Manufacturing Cost	$21,269,890,323.35
Total Cost	$48,637,279,561.41

Then with the total cost, by subtracting out the development and testing costs and distributing the cost over the 120 units necessary from the AIAA requirements, the total flyaway cost ends up being approximately $385,146,000.

3.19.2 Operations and Maintenance Costs (O&M Costs)

The main O&M costs are fuel, crew salaries, and maintenance. Based on historical data, the flying hours for the BWB military transport is determined to be 800 hours per year. The weight of fuel burned per hour by the 4 engines is calculated as:
Weight of fuel burned per hour = TSFC × Thrust required for cruise = 0.4 × 50,000 = 20,000 lbs.

Using the density of Jet-A fuel, which is about 6.75 lbs./gallon; the volume of fuel burned per hour is calculated to be 2,962.96 gallons.

The cost of the fuel is around $5/gallon. Then the fuel cost is calculated as following:
Fuel cost = volume of fuel burned per hour × flying hours per year × fuel price per gallon = 2,962.96 × 800 × 5 = 11,851,851.9 dollars/year

The average basic pay for a U.S Air Force pilot is about $63,000 per year. The total salary that a U.S Air Force pilot will be paid is about four times the basic pay, which is, $252,000 per year. The BWB military transport is designed to have five crews in it. Therefore, the crew salaries will be about $1,260,000 per aircraft per year.

The flyaway unit cost for each aircraft is about $385,145,813. The notional projected lifetime of existing military transport was about 30 years. To be conservative, a life cycle of 20 years was assumed for this aircraft. Then the approximate maintenance costs are calculated to be:[8]

$$\$385,145,813/20 \text{ years} = \$19,257,290/\text{year}.$$

Thus, the Operations and Maintenance Costs (O&M Costs) are:

$$\$11,851,851.9/\text{year} + \$1,260,000/\text{year} + \$19,257,290/\text{year} = \$32,369,142/\text{year}.$$

3.20 Special Considerations

3.20.1 Aerodynamic Special Considerations

Because the BWB military transport is a subsonic airplane, so special aerodynamic considerations, such as isobar tailoring, supersonic area rule, and compression lift do not apply to this airplane.

Special aerodynamic considerations for the BWB military transport will be unexpected separation of the flow and unwanted vortex. Those aerodynamic problems are usually discovered later in real flight tests. If separation of flow and unwanted vortex occur, apparatus such as vertex generator, nose strake will be used if necessary.

References

[1] '463L pallet', http://www.463lpallet.com/, used on 03/13/2015.

[2] 'AH-64 Apache', http://www.boeing.com/boeing/rotorcraft/military/ah64d/, used on 03/13/2015

[3] 'CH-47 Chinook specifications', http://www.boeing.com/boeing/rotorcraft/military/ch47d/ch47dspec.page, used on 03/13/2015

[4] 'FAA Federal Aviation Regulations (FARS, 14 CFR).' *FAR Part § 25.841: [Pressurization]*. N.p., n.d. Web. 12 Apr. 2015.

[5] 'M104 Wolverine AVLB Armored Vehicle-Launched Bridge', http://www.militaryfactory.com/armor/detail.asp?armor_id=734, used on 03/13/2015

[6] Currey, N., 'Aircraft Landing Gear Design: Principles and Practices,' AIAA Education Series, AIAA, Washington, DC

[7] Dommelen, J., 'Conceptual design and analysis of blended-wing-body aircraft,' SAGE, Vol 228, 2014

[8] Haggerty, A., 'Lifecycle Considerations,' Massachusetts Institute of Technology, http://ocw.mit.edu/courses/aeronautics-and-astronautics/16-885j-aircraft-systems-engineering-fall-2004/lecture-notes/lifecycle.pdf

[9] Kuntawala, N., 'Aerodynamic Shape Optimization of a Blended-Wing-Body Aircraft Configuration,' University of Toronto, 2011

[10] Leifsson, L., 'Multidisciplinary Design Optimization for a Blended Wing Body Transport Aircraft with Distributed Propulsion,' MAD Center, Virginia Polytechnic Institute and State University

[11] Liebeck, R., 'Design of the Blended Wing Body Subsonic Transport,' The Boeing Company, Journal of Aircraft Vol 41, 2004

[12] Meier, N, 'Jet Engine Specification Database,' jet-engine.net/civtfspec.html

[13] Mukhopadhyav, V., 'Blended-Wing-Body (BWB) Fuselage Structural Design for Weight Reduction,' Structural Dynamics and Materials Conference, AIAA 2005-2349, Austin TX, 2005

[14] Nikolai, L., 'Fundamentals of Aircraft and Airship Design,' Vol 1., AIAA Education Series, AIAA, Virginia 2010

[15] Raymer, D., *Aircraft Design: A Conceptual Approach*, 5th ed., AIAA Education Series, AIAA,Virginia, 2012

[16] Syed, H., 'A Review of Swept and Blended Wing Body Performance Utilizing Experimental, Fe and Aerodynamic Techniques,' IJRRAS, 2011

[17] Wilfred C. Garrard, *The Lockheed C-5 Case Study in Aircraft Design,* AIAA Professional Study Series

Appendices

The entirety of the appendix will be given on a flash drive. It consists of the excel spreadsheets used to calculate data, meetings notes, and internal communication screenshots.